

3D-Architecture and Neogene Evolution of the Malatya Basin: Inferences for the Kinematics of the Malatya and Ovacık Fault Zones

NURETDİN KAYMAKCI¹, MURAT İNCEÖZ² & PINAR ERTEPINAR¹

¹RS-GIS Laboratory, Department of Geological Engineering, Middle East Technical University, TR-06531 Ankara, Turkey (E-mail: kaymakci@metu.edu.tr)

²Firat University, Department of Geological Engineering, TR-23119 Elazığ, Turkey

Abstract: The 3D-architecture of the Malatya Basin was studied using remote sensing, seismic interpretation, and palaeostress analysis in the context of the Malatya-Ovacık fault zone. The results indicate that the Ovacık and Malatya fault zones are not different segments of a single 'so called' Malatya-Ovacık fault zone; rather, they are two different fault zones that have operated independently. In addition, the Ovacık fault zone is delimited in the west by the Malatya fault zone, which extends farther north from the point of supposed junction. Maximum individual deflection of streams along the Ovacık fault zone is about 9.3 km, and summation of all stream deflections along different segments of the Ovacık fault zone indicates that sinistral displacement of the Ovacık fault zone has been not more than 20 km following development of the drainage system in the region.

Evidence for three different deformation phases were recognized in the Malatya Basin. Deformation phase 1 was characterized by NW-SE-directed extension and operated in the Early to Middle Miocene interval. Deformation phase 2 was characterized by WNW-ESE-directed compression and a vertical σ_2 which indicates transcurrent tectonics. It operated in the Late Miocene to Middle Pliocene. Deformation phase 3 was characterized by NNE-SSW-directed compression, and vertical stress is interchanged with σ_2 and σ_3 ; this is interpreted as due to near equal magnitudes of these stresses, resulting in stress permutation and interchange of intermediate and minor stress. Deformation phase 3 commenced in the Late Pliocene and has been active since then.

The infill of the Malatya Basin has wedge-like geometry in E-W and N-S directions and the basin fed detritus mainly from its eastern margin. During field studies in the basin, a number of inverted normal faults were encountered; these apparently developed as growth faults in the Early to Middle Miocene time interval and then were reactivated or inverted during post-Middle Miocene compressional phases.

Key Words: Malatya Basin, Malatya fault zone, Ovacık fault zone, palaeostress, reactivation, inversion

Malatya Havzasının 3 Boyutlu Mimarisi ve Neojen Evrimi: Malatya ve Ovacık Fay Kuşaklarıyla İlgili Çıkarımlar

Özet: Malatya Havzası'nın 3 boyutlu mimarisi Malatya-Ovacık fay kuşağı bağlamında uzaktan algılama, sismik yorumlama ve paleostres analizleri kullanılarak ortaya konulmuştur. Varılan sonuçlar göstermektedir ki Malatya-Ovacık fay kuşağı olarak adlandırılan hat, tek bir fay kuşağının iki ayrı segmenti olmayıp, aksine bir birinden bağımsız hareket eden iki ayrı fay kuşağıdır. Ayrıca, Ovacık fay kuşağı batı ucunda Malatya fay kuşağı ile birleştiği öne sürülen noktadan daha kuzeye doğru devam eden, Malatya fay kuşağı tarafından sonlandırılmaktadır. Ovacık fay kuşağı içerisindeki derelerin üzerinde görülen en büyük ötelenme 9,3 km olup, derelerin hepsi üzerindeki atım miktarlarının toplamı Ovacık fay kuşağı'nın, bölgedeki akaçlama sisteminin oluşumundan itibaren, toplam ötelenmesinin 20 kilometreden fazla olamayacağını göstermektedir.

Malatya Havzası'nda üç farklı deformasyon evresi tespit edilmiştir. İlk evre KB-GD yönlü bir genişleme dönemi olup Erken ile Orta Miyosen döneminde hüküm sürmüştür. İkinci evre ise σ_2 'nin düşey olduğu ve bölgesel doğrultu atımlı tektonizmaya işaret eden DGD-BKB yönlü bir sıkışma ile temsil edilir. Bu dönem Geç Miyosen ile Orta Pliyosen evresinde hüküm sürmüştür. Üçüncü deformasyon evresi ise KKD-GGB yönlü bir sıkışma altında σ_2 ile σ_3 'ün düşey ekseninde zaman zaman yer değiştirdiği bir deformasyonla temsil edilir. Bu durum iki stres büyüklüğünün eşit olduğu durumlarda görülen stres değiş-tokuşu (permütasyon) olarak yorumlanmış ve ortaç stresle en küçük stresin zaman zaman düşey ekseninde yer değiştirmesinin nedeni olduğu şeklinde yorumlanmıştır.

Üçüncü deformasyon evresi, Geç Pliyosende başlayıp günümüze değin etkisini sürdürmektedir.

Malatya Havzası'nın dolgusu D-B ve K-G yönünde kama şeklinde bir geometriye sahip olup genelde doğu kenarından beslenmiştir. Arazi çalışmaları sırasında, havzada bir çok terselmiş faylara rastlanmıştır. Bu fayların Erken-Orta Miyosen döneminde büyüme fayları olarak gelişip Orta Miyosen sonrası sıkışma dönemlerinde yeniden hareket kazandıkları veya terseldikleri oldukça belirgindir.

Anahtar Sözcükler: Malatya Havzası, Malatya fay kuşağı, Ovacık fay kuşağı, paleostres, tekrar hareketlenme, terselme

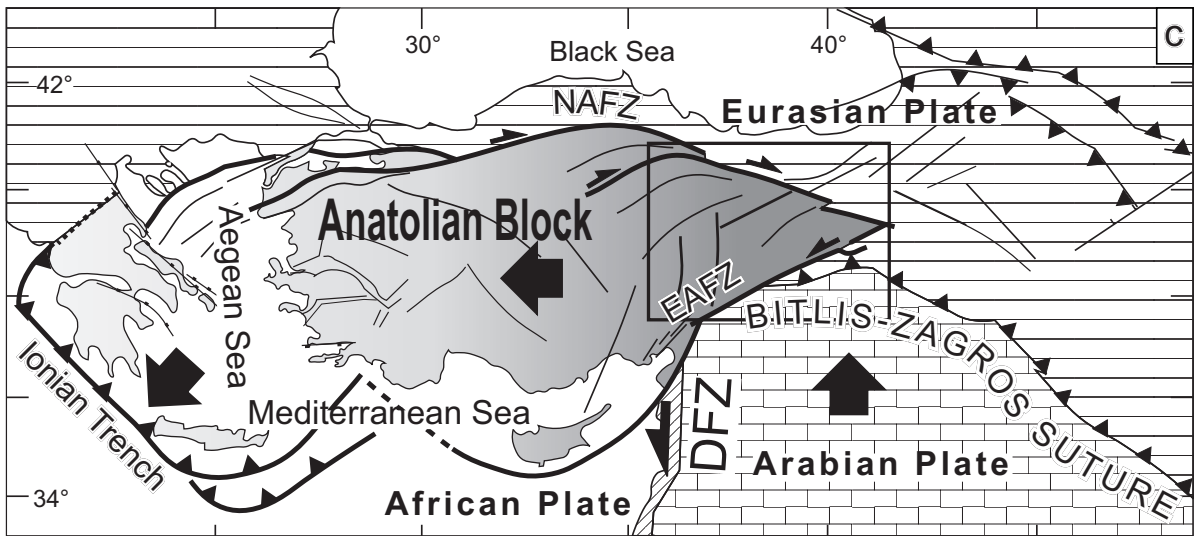
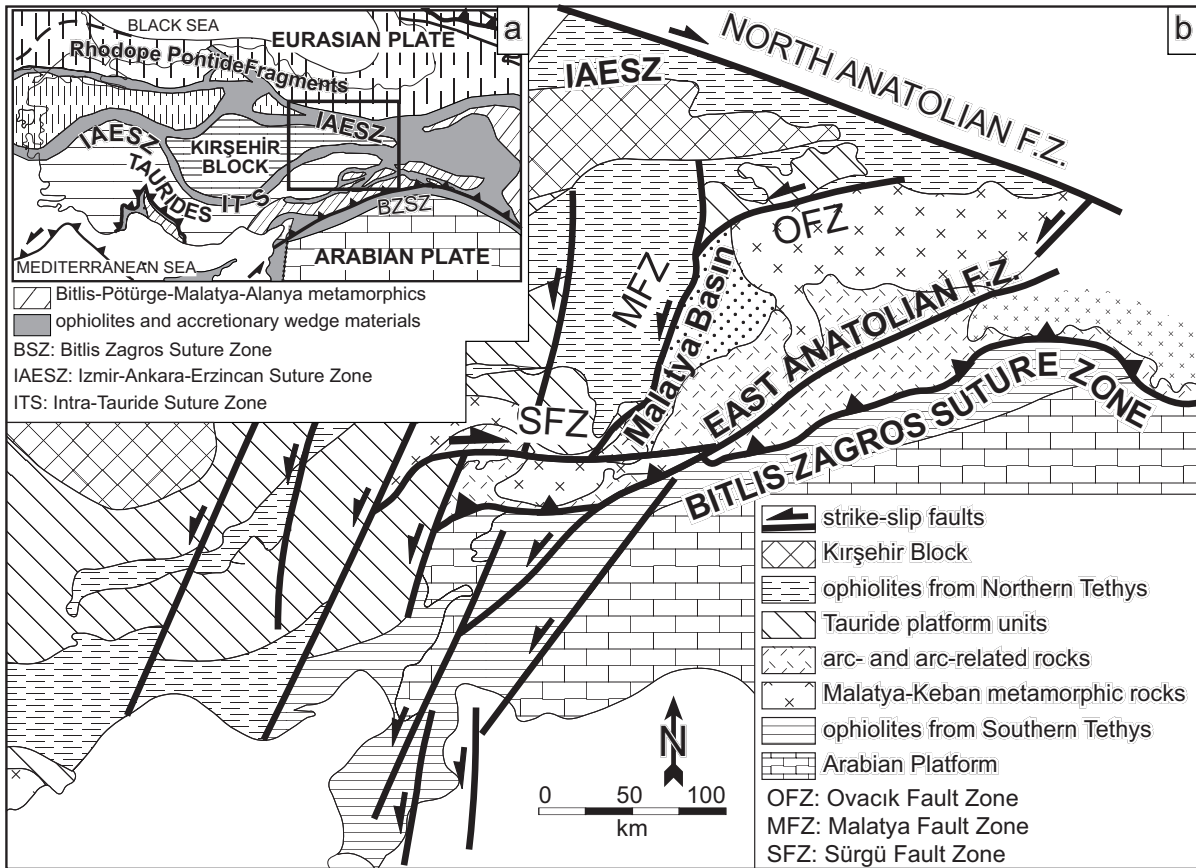
Introduction

The Late Cretaceous to early Tertiary evolution of Turkey was dominated mainly by northward subduction along the northern and southern branches of the Neotethys Ocean and collision processes after their terminal closure. The northern branch is located between the Rhodope-Pontide fragments in the north and the Taurides in the south (Figure 1a). The southern branch was located between the Eurasian and Arabian plates in SE Turkey (Şengör & Yılmaz 1981; Görür *et al.* 1984; Yılmaz *et al.* 1993; Koçyiğit & Altın 2002). Complete subduction and obliteration of the former took place in the Late Cretaceous to early Tertiary (Yalınz & Göncüoğlu 1999; Gençalioglu-Kuşçu *et al.* 2001; Rojay *et al.* 2001) which resulted in collision of the Taurides and Pontides along the İzmir-Ankara-Erzincan Suture Zone (Şengör & Yılmaz 1981; Koçyiğit 1991; Kaymakçı 2000; Kaymakçı *et al.* 2000, 2003a, b) during the early Tertiary. Terminal subduction and obliteration of the southern branch took place along the Bitlis-Zagros Suture Zone in the Late Miocene (Şengör & Yılmaz 1981; Şengör *et al.* 1985; Dewey *et al.* 1986; Yılmaz *et al.* 1993) and resulted in the collision of the Arabian plate with the Eurasian plate. The collision and further northward convergence of the Arabian plate gave way to the westward escape of the Anatolian Block along the dextral North Anatolian and sinistral East Anatolian fault zones (NAFZ and EAFZ, respectively) from the zone of high convergent strain towards the Aegean trench. Although there is debate about the timing of collision and the inception of the NAFZ and the EAFZ, the neotectonic scheme of Turkey is relatively better known than the geological constraints that existed before the Arabian collision took place. This is partly due to difficulties in the dating of continental deposits which prevailed in most of the early Tertiary and the Neogene, and partly due to the lack of regional studies addressing this problem, in addition to incomplete kinematic and tectono-stratigraphic studies in the basins

that might contain complete records of the subduction, collision and post-collisional processes.

The Malatya Basin is one of the largest basins in eastern Turkey (Figure 2). It is located in the hinterland of the Bitlis-Zagros Suture Zone (Figure 1b) which demarcates the former position of the southern branch of the Neotethys, and along which the Arabian and Eurasian plates collided (Figure 1c). It has infill more than 2 km thick spanning the Early Miocene to Recent, and which rests on Lower Tertiary volcano-sedimentary units. Therefore, it offers a unique opportunity for understanding the Neogene development of the region as well as the effects of collision and post-collisional convergence to which this paper is addressed. Therefore, the primary aim of this paper is to describe and model the 3D-architecture of the Malatya Basin and to unravel its Neogene evolutionary history using remote sensing, seismic interpretation and palaeostress inversion based on fault-slip data. The information obtained from the Malatya Basin will be used to understand the development and evolution of the region, especially the kinematics and activity of the two major fault zones of the region, namely the Malatya and Ovacık fault zones (MFZ and OFZ, respectively). Field studies included 'ground-truthing' of remotely sensed information and seismic interpretation, and evaluation of large-scale structures and fault kinematics based on palaeostress analysis from fault-slip data sets collected during field studies. In addition, the information obtained from the Malatya Basin will be extrapolated to constrain and discuss the possible active tectonics and deformation mechanisms of the region.

A brief stratigraphic summary of the region with special emphasis on the Neogene infill is given first, and followed by remote sensing, seismic interpretation and palaeostress analysis, and finally by a discussion of the data and our conclusions.



active convergence zones
 major strike-slip faults
 subordinate faults

DFZ: Dead Sea Fault Zone, EAFZ: East Anatolian Fault Zone, NAFZ: North Anatolian Fault Zone

Figure 1. (a) Palaeotectonic outline of Turkey (modified from Şengör *et al.* 1984 and Görür *et al.* 1984); (b) isopic zones of the eastern Taurides (modified from Perinçek & Kozlu 1984); (c) neotectonic outline of Turkey and surrounding regions (reproduced from Kaymakçı 2000).

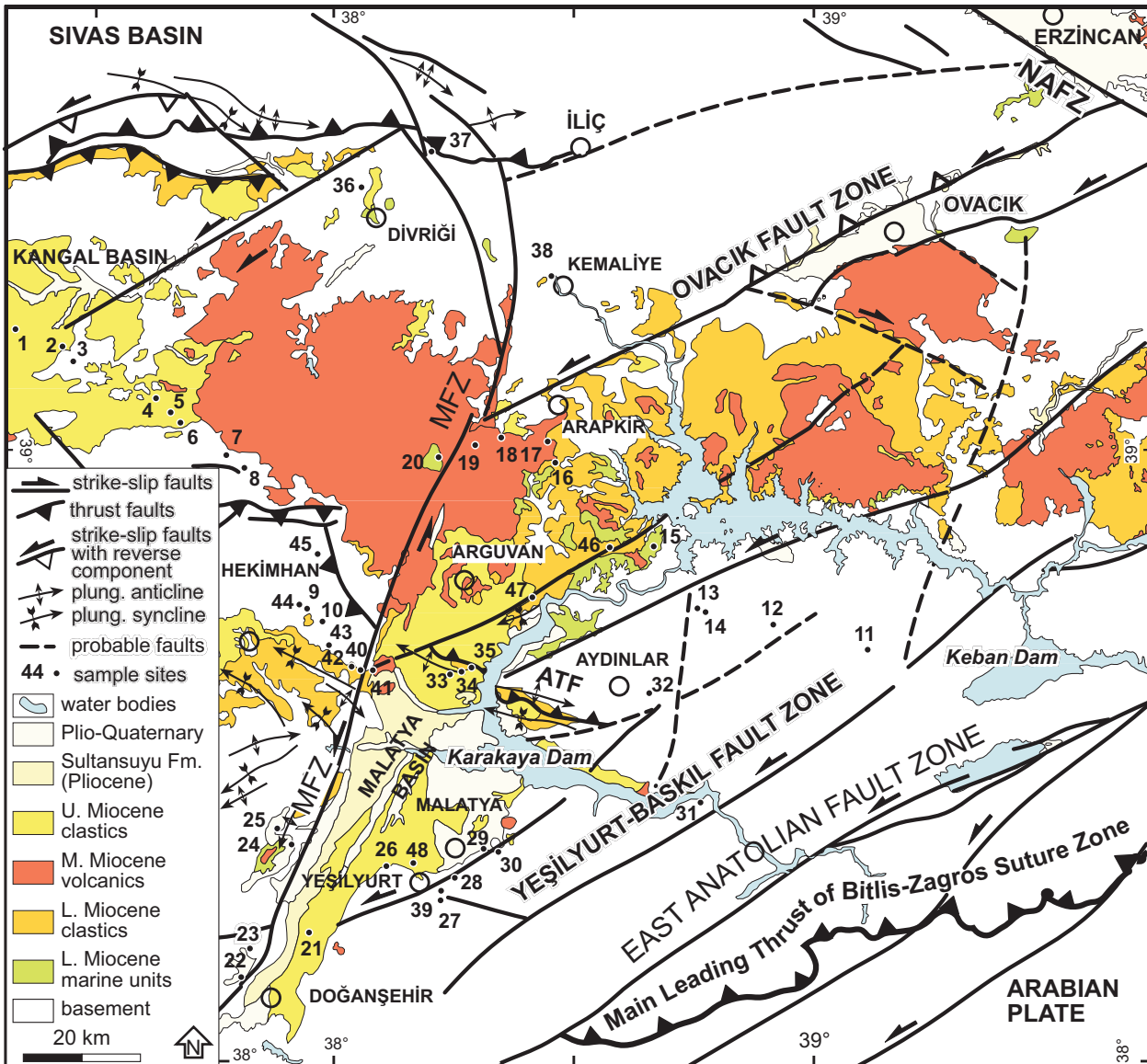


Figure 2. Geological map of the Malatya Basin area for the Neogene.

Stratigraphy

The lithologies exposed in and around the Malatya Basin are grouped as basement rocks – upon which the basin has developed – and as basin infill. All of the pre-Neogene units are designated basement since their deposition predates the development of the Malatya Basin and are not confined to the area within the boundaries of the basin (Figure 2). Field studies and seismic interpretations indicate that basin development has been accompanied by extensional deformation which commenced in the Early

Miocene. In fact, the actual development of the Malatya Basin succeeded Early Miocene regional extension which gave way to widespread deposition in E and SE Anatolia far beyond the present boundaries of the Malatya Basin and was accompanied by marine incursions. Therefore, the Early Miocene units are also included in the basin infill (Figure 3). Although they are not confined to the present limits of the Malatya Basin, they are related to the extensional deformation which stimulated basin development.

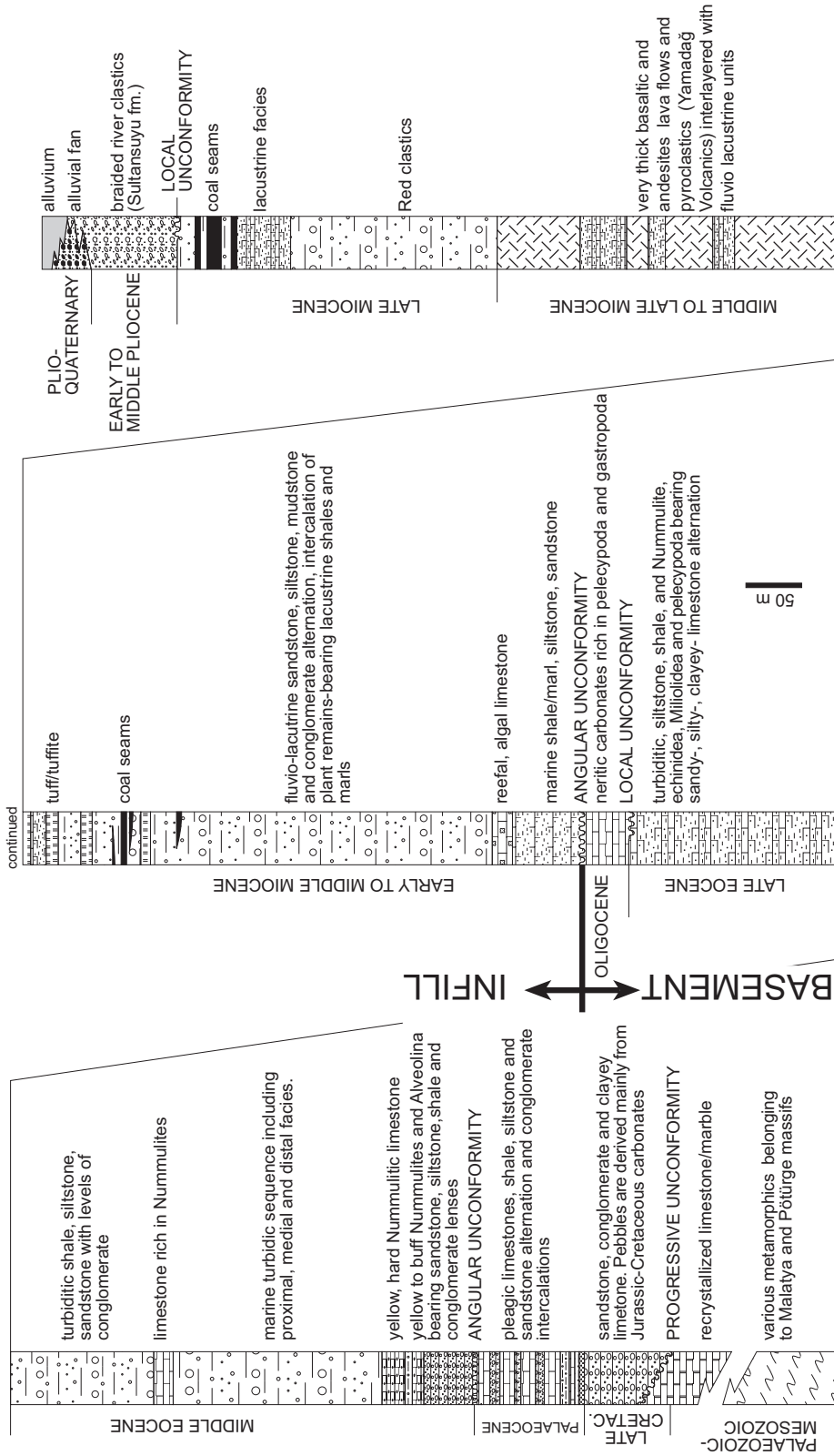


Figure 3. Generalized columnar sections for the basement and the infill of the Malatya Basin (modified from Sümençen & Uysal 1990).

Basement Units

The present study focuses on the Neogene development of the Malatya Basin; detailed description of the basement units is beyond the scope of this work. However, a brief summary of the basement units will be given below.

The geology of the basement units is not yet fully understood. In the literature (references herein), there are different models and scenarios that have been set forth to explain the evolution of the region. Among these, the most comprehensive is the one of Perinçek & Kozlu (1984) upon which our summary is based. The basement in the region comprises various metamorphic rocks, Mesozoic platform carbonates, Late Cretaceous ophiolitic slivers and mélanges, various Late Cretaceous to Early Palaeocene volcanic rocks and volcano-sedimentary assemblages, Late Palaeocene to Oligocene volcanoclastic, marine clastic, and carbonate rocks, and widespread evaporite occurrences (Figure 3). These units were intruded by various intrusive igneous bodies in the early Tertiary. Regionally, the basement units are included in the eastern Tauride belt. Perinçek & Kozlu (1984) subdivided the basement units according to the isopic zones of Özgül (1976) and Özgül & Turşucu (1984) in the central Taurides (Figure 1b).

The tectonic development of the region was dominated mainly by the southward thrusting of ophiolite masses originating from the northern Neotethys along the İzmir-Ankara-Erzincan Suture zone (Figure 1a) in the Late Cretaceous, and northward thrusting and ophiolite obduction originating from the Intra-Tauride Ocean from which arc and arc-related intrusive and volcanic rocks originated in the early Tertiary. In addition, some of the ophiolitic units obducted along the south-verging thrust sheets over the Arabian plate originated from southern Tethys in the late Tertiary to Late Miocene (Perinçek & Kozlu 1984; Aktaş & Robertson 1984; Yazgan 1984; Yılmaz *et al.* 1993).

The early Tertiary units in and around the basin are characterized by various microfossil-, pelecypod- and gastropod-bearing limestones intercalated with alternations of turbiditic sandstone, siltstone, shale and marl (Figure 3). These units are capped along a local unconformity by Oligocene neritic carbonates rich in pelecypods and gastropods. All of the early Tertiary units are unconformably overlain by the Lower Miocene infill of the Malatya Basin.

We refer the reader to Bingöl (1984), Perinçek & Kozlu (1984), Özgül & Turşucu (1984), Yazgan (1984), Aktaş & Robertson (1984), Kozlu (1987), Yılmaz *et al.* (1993), Robertson (2002), Jaffey & Robertson (2004), and Robertson *et al.* (2004, 2005) for a full description of the basement units and, mainly, interpretations of the early Tertiary evolution of the region.

Infill

The infill of the Malatya Basin rests unconformably on the Oligocene and older units and begins, at its base, with buff to yellow and white clayey marine sandstones, siltstones and marl, and continues upward with an algal fossiliferous limestone, turbiditic, fining-upward sequences of sandstone, siltstone and shale, and intercalations of thickly bedded marls (Olukkaya Formation of Sümengen & Uysal 1990). This unit marks the onset of marine inundation in the region after early Tertiary compression generated thickening and uplift of the region (Perinçek & Kozlu 1984; Yılmaz *et al.* 1993). This unit has been dated by various researchers (e.g., Perinçek & Kozlu 1984; Yalçın & Görür 1984) who have reported that it is of Early Miocene to Middle Miocene age. These marine units are conformably overlain by continental fluvio-lacustrine assemblages at the centre of the basin, while at the basin margins they are locally overlain unconformably by Middle Miocene continental units. The Middle Miocene fluvio-lacustrine assemblage (Zeynepoğlu Formation of Sümengen & Uysal 1990) is exposed mainly in the central and northern parts of the Malatya Basin. The thickest and relatively most complete sections of these units are exposed in the central part of the Malatya Basin – south of the Aydınlar thrust fault – in the core of an anticline (location 35 in Figure 2) and are composed of (in decreasing abundance) lacustrine, marl, shale, siltstone and sandstone, and includes various currently economic coal horizons intensely sheared by thrusting with a top-to-north vergence. In the northern part of the Malatya Basin, these lacustrine units are interlayered with various lava flows and pyroclastic materials of the Yamadağ volcanics. The radiometric ages of interlayered volcanic rocks (Leo *et al.* 1974; Arger *et al.* 2000) are late-Early to Middle Miocene (ca. 18 to 14 Ma). In the NW part of the Malatya Basin, N of Arguvan (Figure 2), the Yamadağ volcanic rocks separate the Malatya Basin from the Kangal Basin and are intercalated with and overlain by a few tens of meters of thick red

clastics which are also exposed in the Kangal Basin and are overlain by an approximately 100-m-thick lacustrine sequence with economic coal horizons. Continental mammalian fossils collected from these units have been dated by Hans de Bruijn (Faculty of Geosciences, Utrecht University, The Netherlands). The following faunal elements were identified from Kangal Basin: *Talpidae Desmaninae*, *Archaeodesmana*, *Insectivora Soricidae*, *Sciuridae Tamias*, *Gerbillinae Pseudomeriones*, *Cricetinae s.l. Blancomys*, *Murinae Micromys*, *Murinae Occitanomys*, *Spalacinae Pliospalax*, *Castoridae Dipoides*, *Eomyidae Keramidomys*, *Cricetinae Allocricetus*, *Murinae Apodemus*, *Ochotonidae Prolagus*, *Hyaenidae Perissodactyla Equidae Hipparion*, and *Proboscidea Gompotheriidae Anancus*. These fossils characterize the European MN-13 Mammal Zone. In addition, *Progonomys* sp. was identified in samples collected from the central part of the Malatya Basin (site 35). It was the first real mouse (Murinea) to arrive in Europe and the Middle East and characterizes MN 9 and younger zones. Similar fauna have also been observed in different parts of the Kangal and Sivas basins (Saraç *et al.* 2000); therefore, a Late Miocene age can be assigned to the upper levels of the infill of the Malatya Basin.

In the southern part of the Malatya Basin, the Late Miocene units are overlain by very thick fluvial (mainly braided river) conglomerates and sandstones (the Sultansuyu formation, first named in the present study). However, no fossils could be identified in these units. A faunal assemblage comprising *Arvicolinae Promimomys/Mimomys*, *Rodentia Eomyidae*, *Castoridae Castor praefiber* and *Gerbillinae* was identified by Sickenberg (1975) in a similar facies of the Elbistan Basin (located approximately 50 km W of the Malatya Basin). In addition, Ünay & Bruijn (1998) reported *Rodentia Castoridae*, *Murinae Apodemus cf. Dominans*, *Arvicolinae Mimomys Moldavicus* and *Insectivora Soricidae*, *Cricetinae Mesocricetus aff. Primitivus*, *Spalacinae*, *Murinae Occitanomys cf. Brailioni*, *Murinae Apodemus Dominans*, *Arvicolinae Mimomys occitanus*, and *Lagomorpha Ochotonidae Ochotonoides* from two different localities at the western margins of the Elazığ Basin which has facies characteristics similar to those of the Sultansuyu formation. These fossils characterize the MN14-15 European Mammal zones. Based on this information, an Early to Middle Pliocene age is assigned to the Sultansuyu formation.

The Sultansuyu formation is unconformably overlain by various alluvial-fan deposits exposed mainly along the Malatya fault zone and the eastern margin of the Malatya Basin. Although no age data have been reported from these units, based on their stratigraphic position over the Sultansuyu formation, a post-Middle Pliocene age is assigned to these alluvial-fan deposits.

The youngest deposits of the Malatya Basin are actively accumulating alluvium and alluvial-fan deposits along active faults, mainly in the southern part of the Malatya Basin around Doğanşehir.

Remote Sensing

Remote-sensing studies have included processing and interpretation of Landsat TM, Space Shuttle Topographical Mission (SRTM) data and Advanced Spaceborne Thermal Emission Radiometer (ASTER) images. SRTM was used to produce a digital terrain/elevation model (DTM/DEM) of the topography.

These images have different levels of spatial (ground) resolution and spectral resolution (i.e., bands). For example, Landsat images have a 30-m ground resolution while the SRTM data is at 3 arc seconds (approximately 69.18 m in the E–W direction and 92.46 m in the N–S direction) resolution; these were used to produce a digital terrain (elevation) model of the region. These images are quite useful for detecting large-scale structures, but they fail to detect structures less than their spatial resolution. Out of 14 bands, the first three VNIR (visible and infrared) bands of the ASTER imagery have a 15-m ground resolution; these were used in areas where higher ground resolution is needed. The SRTM is used to visualize the topography of the region (Figure 4a). This method enhances the detection of lineaments and structures, including active faults of the region. After the images were enhanced and lineaments were delineated visually on the images, delineated lineaments were checked during field studies. The lineaments lacking the field expression were removed, and existing lineaments were labelled as faults; also, fault-slip data were collected from most of these faults. The enhanced image and resultant map are given in Figure 4.

On the images and in the field, it was observed that the Malatya fault zone is composed of a number of sub-parallel strands (Figure 4b, c). In general, the MFZ displays an anastomosing pattern characterized by small

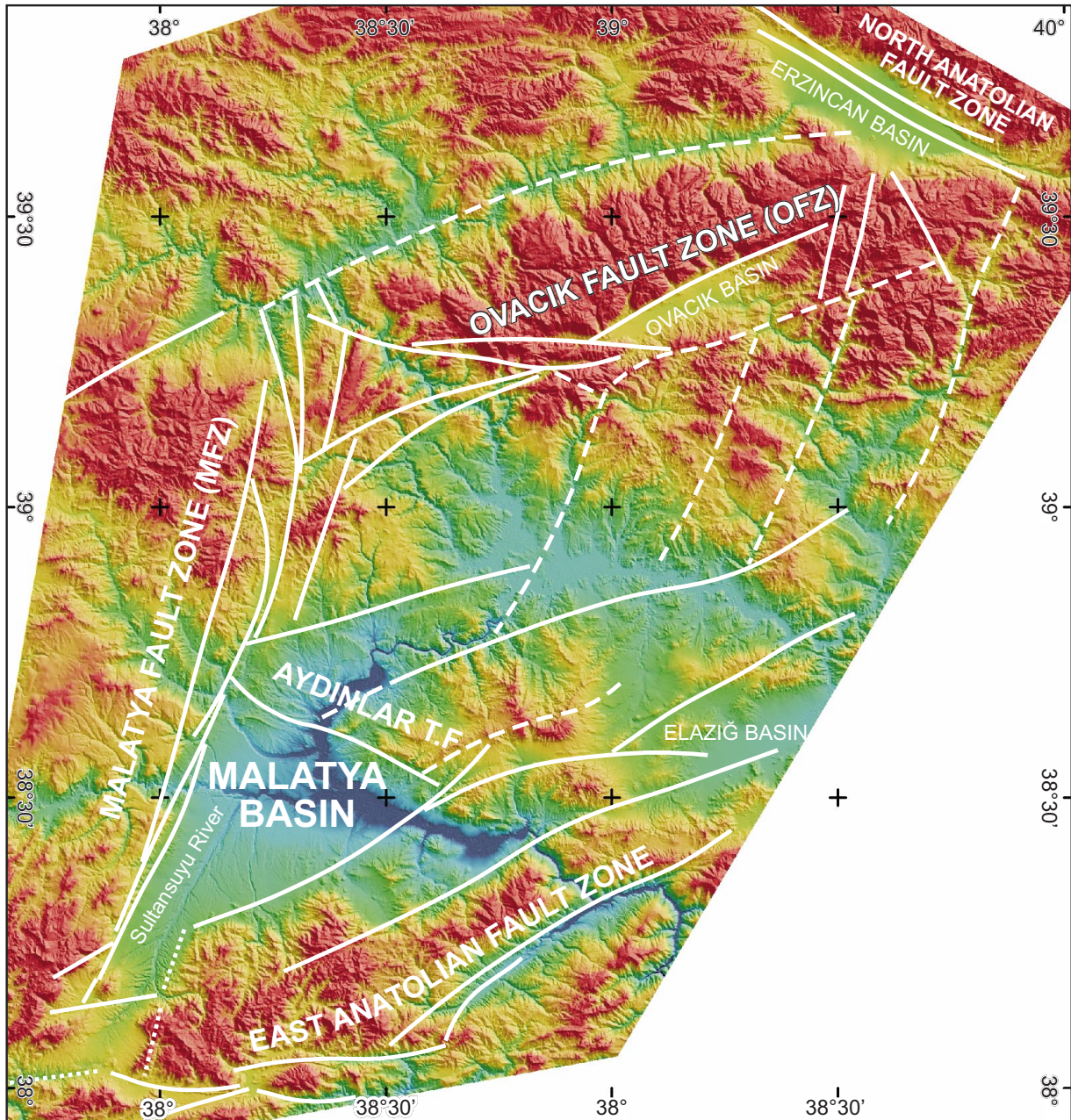


Figure 4. (a) Colour-coded shaded relief image of Malatya Basin area prepared from SRTM data and major lineaments in the region. Note that the Ovacik fault zone is delimited by the Malatya fault zone. Note also the very straight course of the Sultansuyu River; (b) structural map of the Malatya basin, produced from field and remote-sensing studies. Note displaced stream channels (indicated by blue arrows). (c) structural elements and offset streams are overlaid on ASTER imagery.

local highs and depressions, linear valleys and deflected streams; these features are characteristic of strike-slip fault zones. The MFZ delimits the western margin of the Malatya Basin with a pronounced escarpment that

reaches an elevation of 600 m above the Plio–Quaternary floor of the Malatya Basin (Figure 4a). In the northern part of the Malatya Basin, the western continuation of the Ovacik fault zone is has been traced.

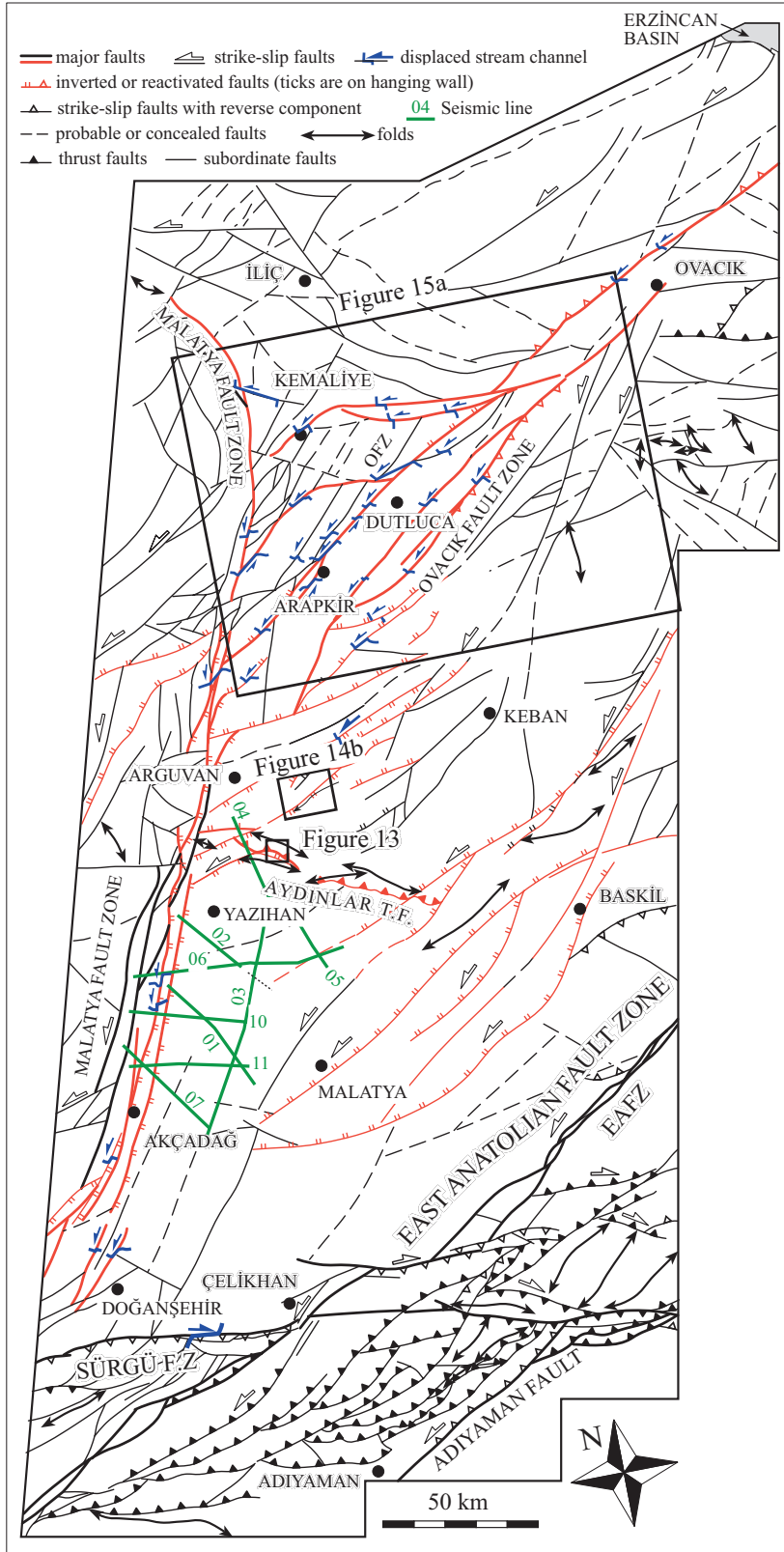


Figure 4b.

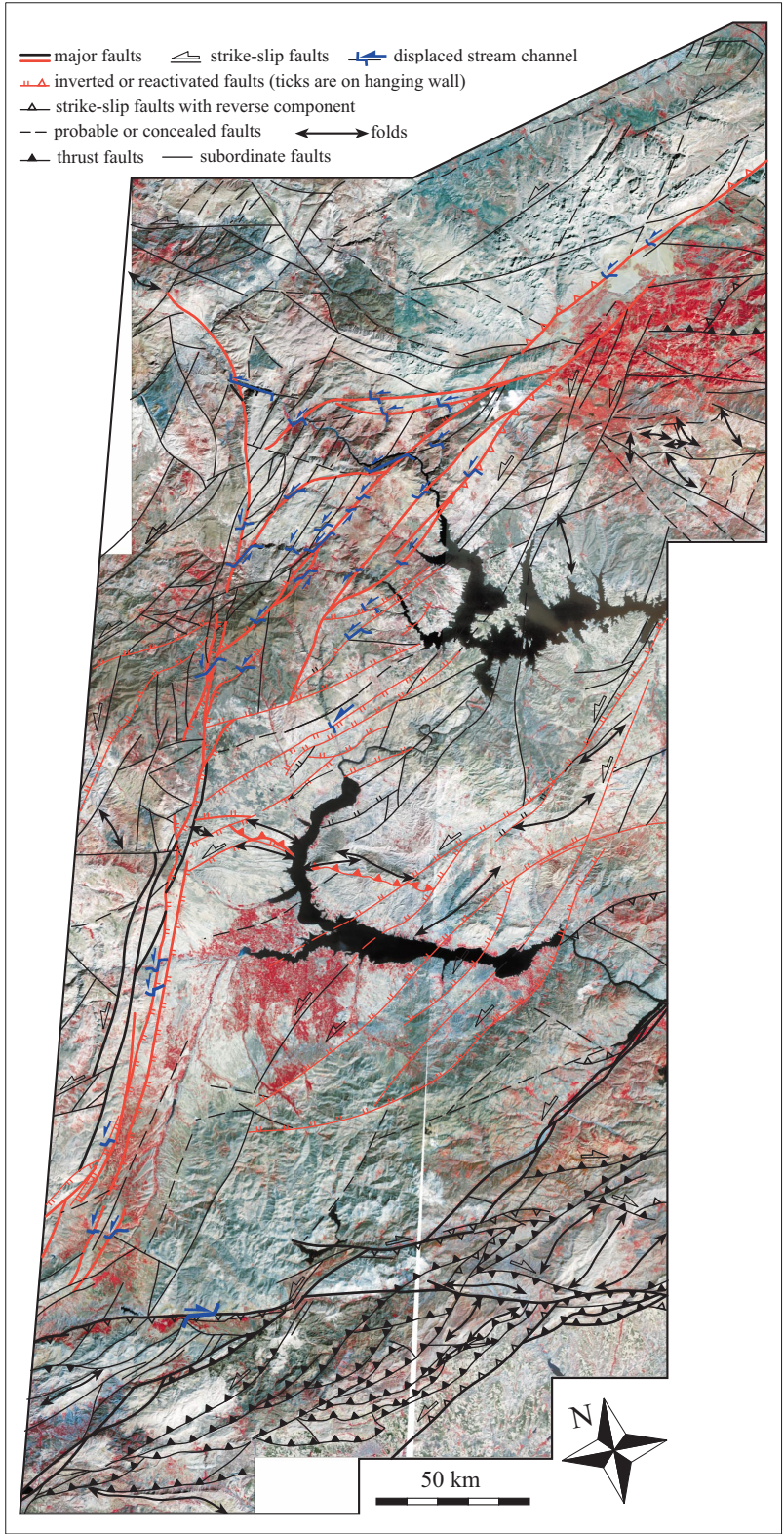


Figure 4c.

Seismic Interpretation

Out of 11 sections, nine seismic lines that were shot by Mobil Exploration Mediterranean Inc. in 1990 were obtained from the Turkish General Directorate of Petroleum Affairs. The available seismic lines are in time domain and were stacked by the company. The interpretation of the sections was performed manually, directly onto the hard copies. During the interpretation, the boundaries of stratigraphic horizons and exposed faults were extrapolated from outcrops.

In the seismic sections, Eocene to Oligocene sequences, pre-Eocene units, Early Miocene marine limestones, Early to Late Miocene units and Plio–Quaternary sequences were identified. The lines O1, O2, O6, O7, O10 and O11 (see Figure 4b for their locations) traverse the western margin of the Malatya Basin, and the Malatya fault zone has been interpreted along these lines (Figures 5–10). The other lines, including O3, O4 and O5 (Figure 11), were shot directly in the Malatya Basin and do not cross the Malatya fault zone. It has been observed that the MFZ displays a positive flower structure (cf. Sylvester 1988), a feature typical of strike-slip fault zones (Figure 12). Different branches of the flower structure have both reverse and normal components of slip, while the strike slip is the dominant slip sense. In all of the seismic sections, some subordinate faults were also interpreted. In the combined sections of lines O4 and O5 (Figure 11), the Aydınlar thrust fault (ATF) has been recognized, which was also observed during field studies (Figure 13a). It is noted that most of the secondary faults in the Malatya Basin, including the ATF, are reactivated normal faults. Among these, the most spectacular inverted fault is observed in relation to the Aydınlar thrust fault. In the southern part of the ATF (on the hanging-wall block), the Early to Late Miocene infill of the Malatya Basin is quite thick, while it is extremely thin on the northern block; this indicates a typical normal growth-fault pattern. Along the inverted fault near the ATF, the basal limestone facies (Early Miocene reefal limestones) and overlying units are up-thrown. Collectively, this information indicates that the first normal faulting occurred, then the normal fault was inverted. During inversion of the ATF, a roof thrust developed which resulted in formation of a triangular zone (Figure 13b). Moreover, an anticline developed due to bending of the inverted fault along the pre-existing

normal fault plane. Similar inversion patterns are also observed all along the MFZ (Figures 5–12).

Palaeostress Analysis

From 49 sites, 696 fault-slip data were collected. The sampled horizons range from Late Cretaceous to Plio–Quaternary in age. Therefore, we have a complete record of deformation since the Late Cretaceous.

Palaeostress configurations were constructed using Angelier's software. During the analysis of the fault-slip data, a methodology developed by Kaymakçı (2000) and Kaymakçı *et al.* (2000, 2003a) was followed. The main steps in the palaeostress analysis were: (1) separation of deformation phases in the field; (2) an automated separation process was applied using the grid search method (Hardcastle & Hills 1991) because of the possibility of mixed data sets; (3) misfit faults were separated from the bulk data and were analyzed separately [This process was applied until reliable results were obtained. 'Reliable results' means that all the faults in one set can have 15° of maximum deviation (ANG of Angelier 1988, and that the maximum value of the quality estimator (RUP) is 45° (see Angelier 1994)]; (4) the faults which did not fulfil these conditions were regarded as spurious, possibly due to measurement errors [After the analysis of the data, it was found that less than 1% of the data were spurious, or about 12 faults; the remaining 684 faults yielded reliable stress configurations. At some of the sites, more than one deformation phase was recognized in addition to separation in the field; they were then separated and re-processed]; (5) 56 different stress configurations were then constructed; among the 56 stress configurations, 41 of them belong to Miocene to Recent deformation phases since their data were collected from Neogene units. The resultant stress configurations are depicted in Figure 14 and in Table 1. [The remaining 15 stress configurations were collected from Late Palaeocene to Oligocene syn-sedimentary faults, thought to belong to pre-Miocene deformation phases. Therefore, those data are presented elsewhere and are not included in this paper]; and (6) the constructed stress configurations were grouped according to their ages. Dating of events is based on the ages of the hosting formations and the relative order of occurrences as discussed in the next section.

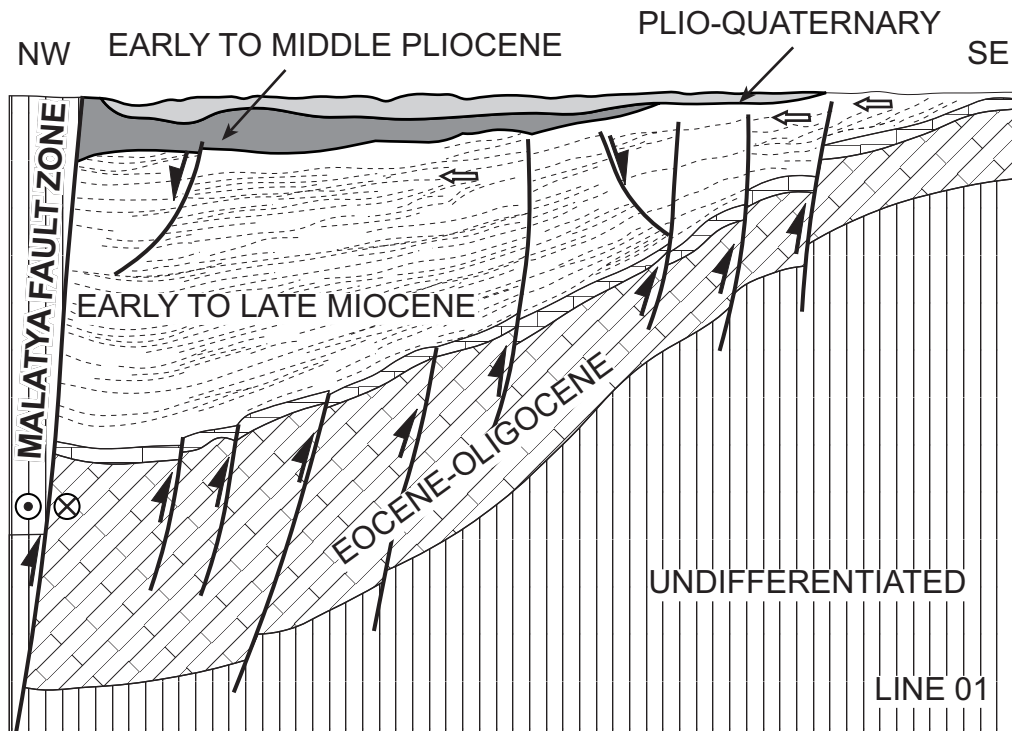
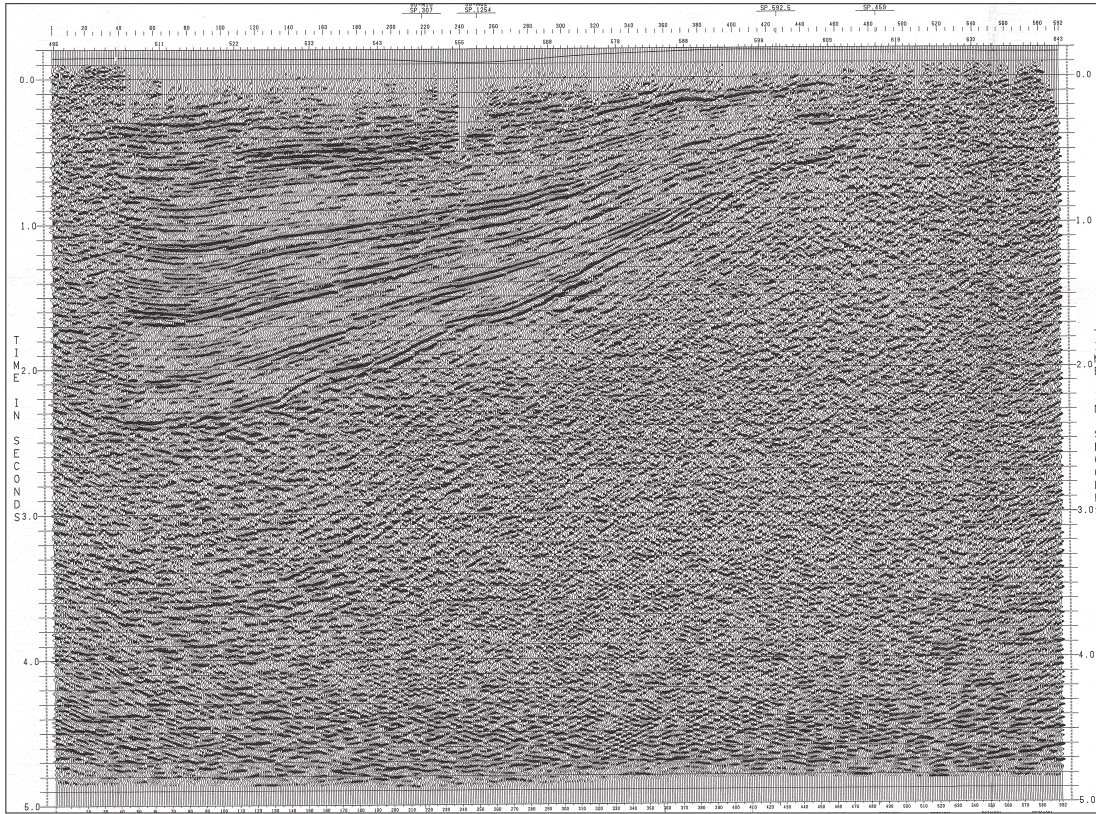


Figure 5. Uninterpreted and interpreted seismic section along line 01. Arrows mark fore-sets and/or shingles that indicate sediment transport direction. MFZ- Malatya fault zone. See Figure 4b for location.

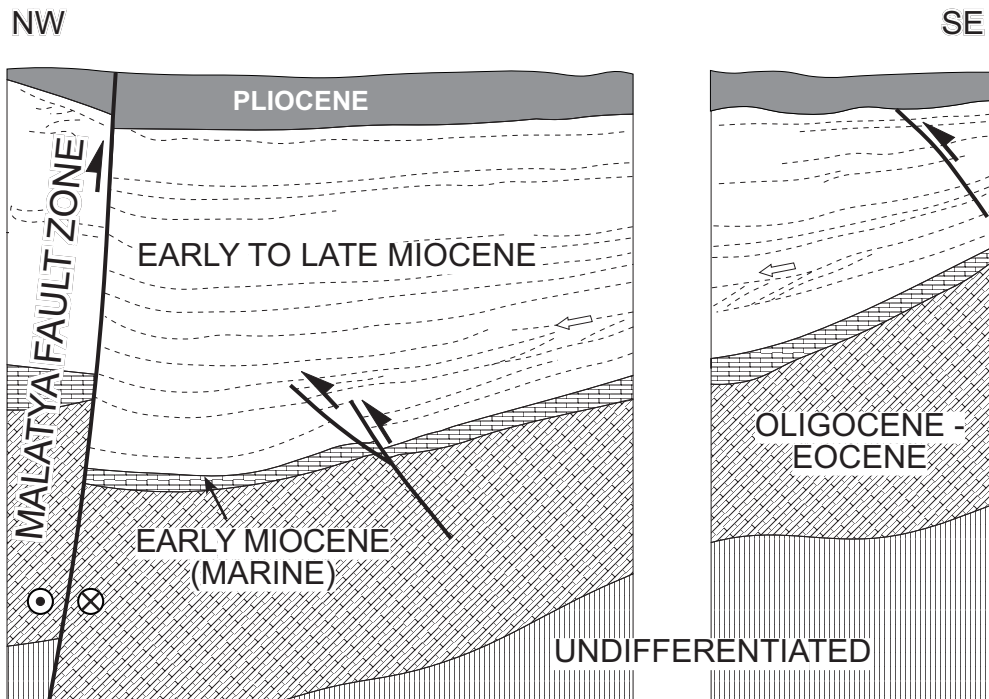
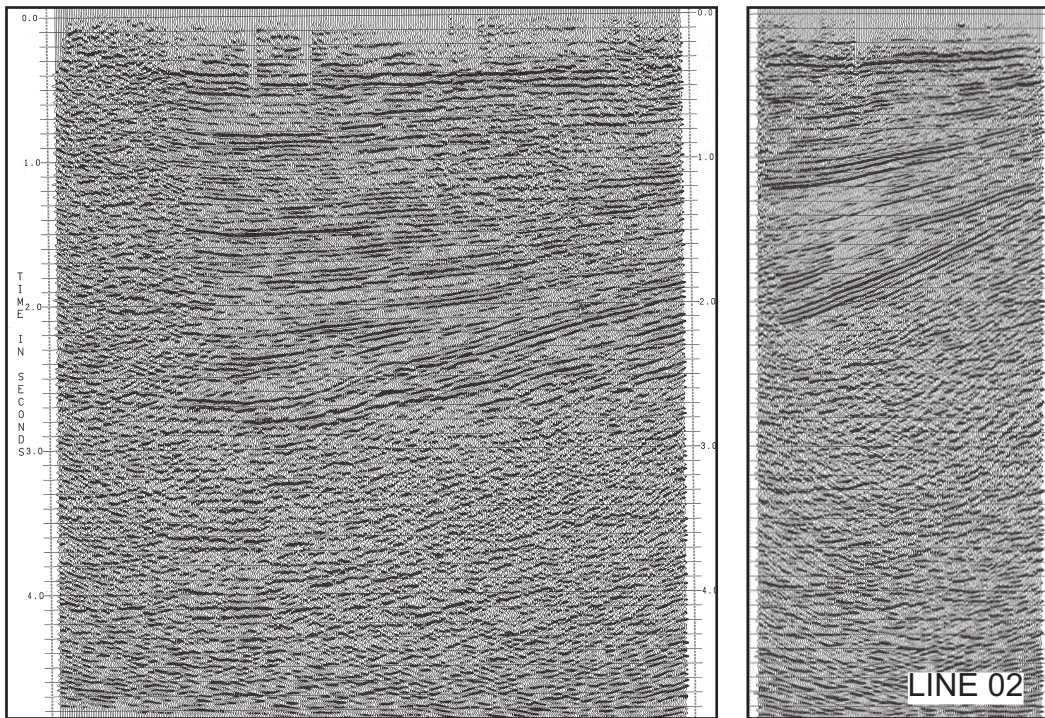


Figure 6. Uninterpreted and interpreted seismic section along line 02. Arrows mark fore-sets and/or shingles that indicate sediment transport direction. MFZ– Malatya fault zone. See Figure 4b for location.

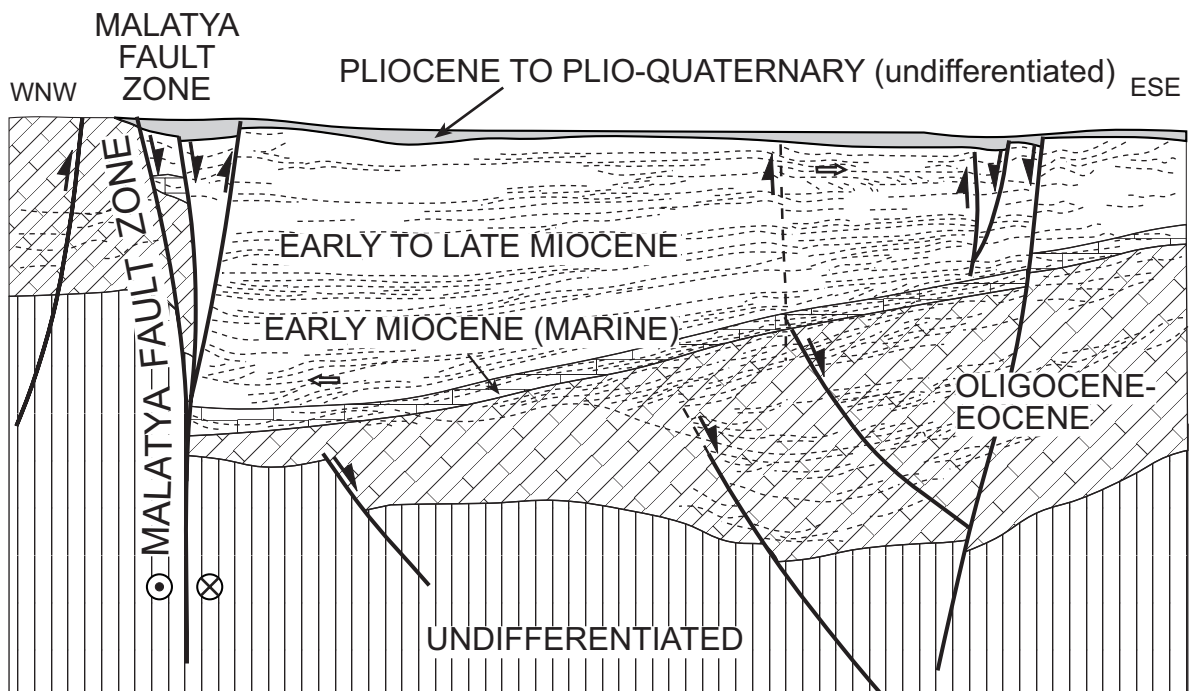
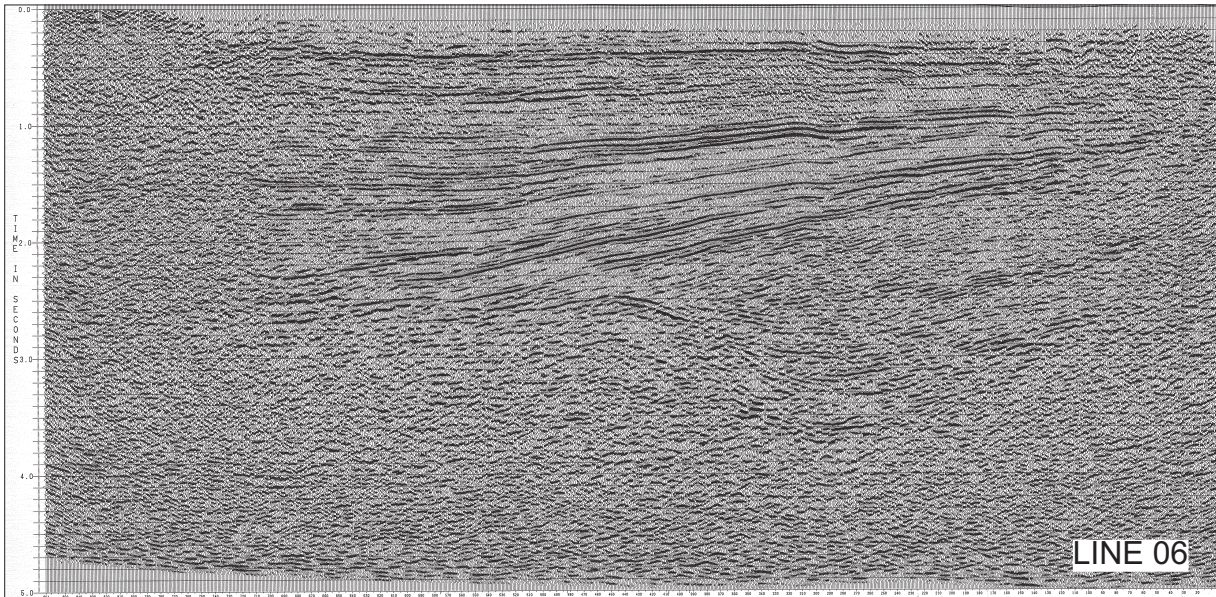


Figure 7. Uninterpreted and interpreted seismic section along line 06. Arrows mark fore-sets and/or shingles that indicate sediment transport direction. MFZ– Malatya fault zone. See Figure 4b for location.

Field Observations and Deformation Phases

During field studies, various compressional and extensional structures were observed at different stratigraphic horizons. This information, together with

overprinting slickensides and block tilting, were used to differentiate the deformation phases. The most reliable results for ordering the deformation phases were based on mesoscopic faults sealed by strata that are unaffected by them.

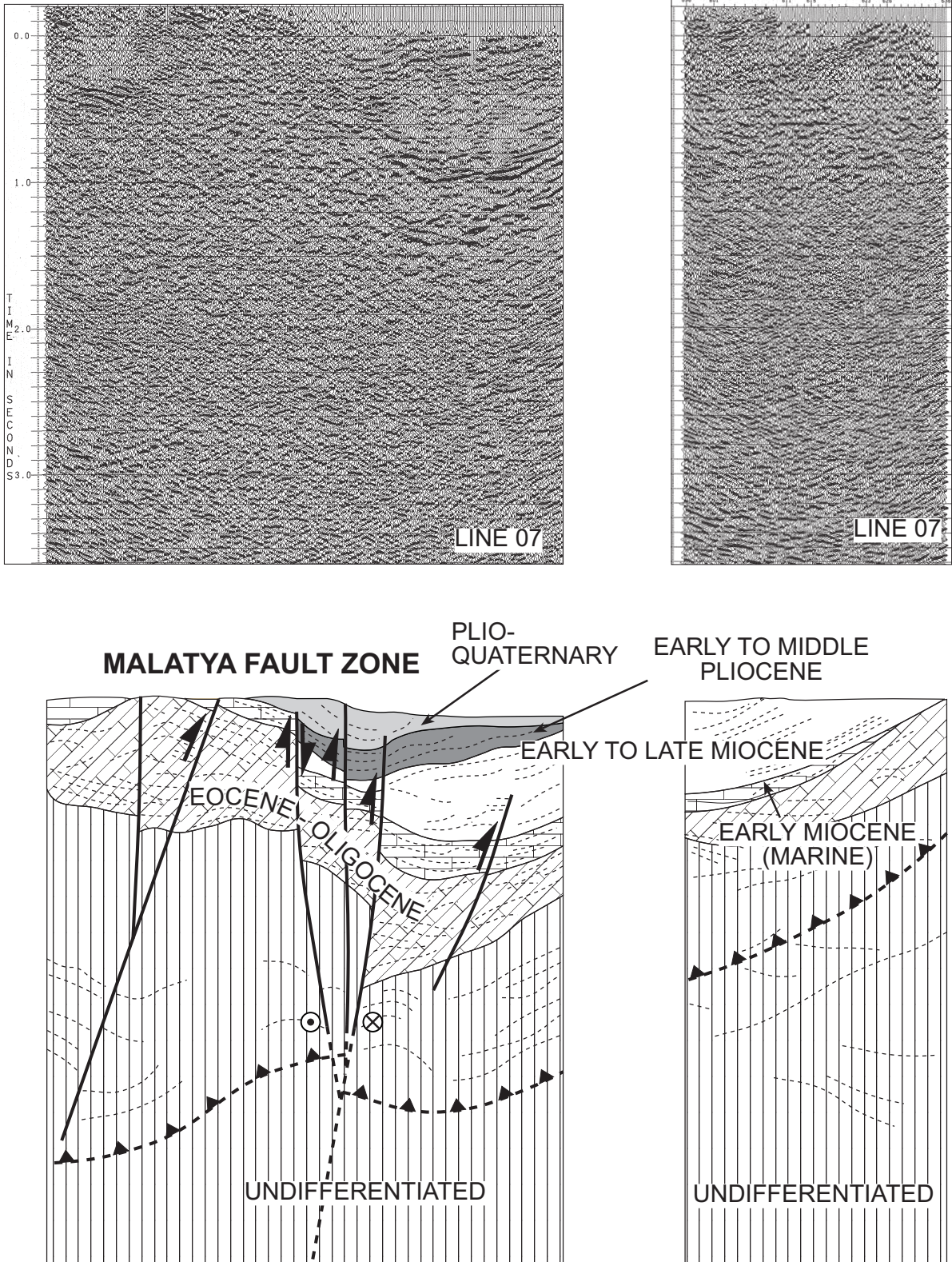


Figure 8. Uninterpreted and interpreted seismic section along line 07. MFZ– Malatya fault zone. See Figure 4b for location.

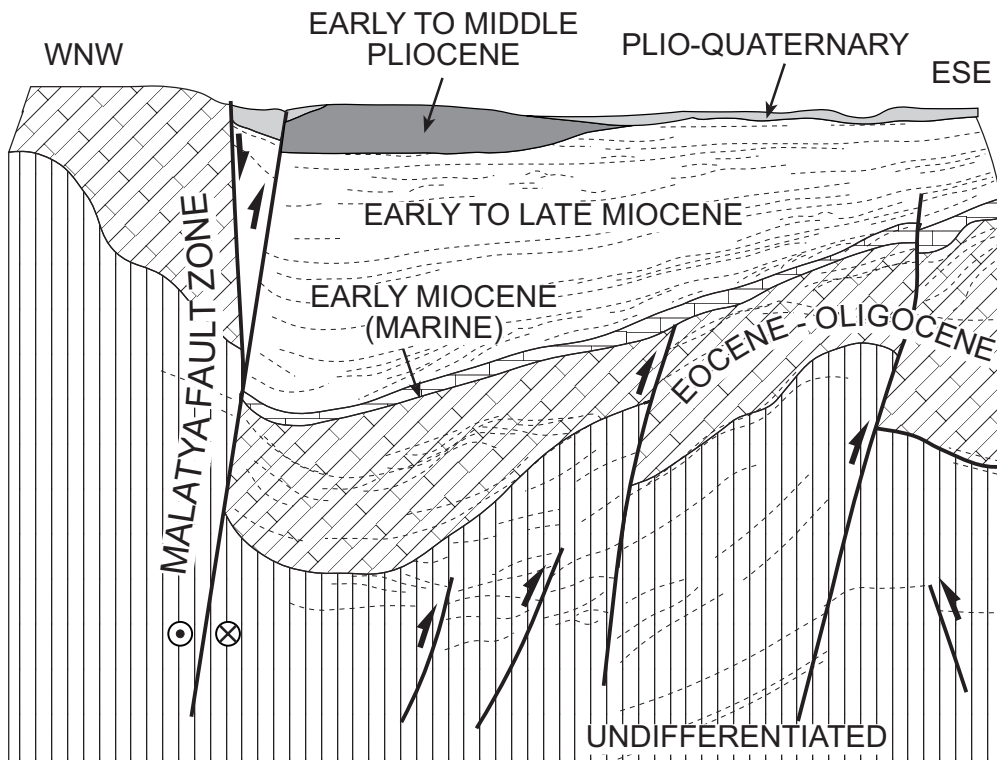
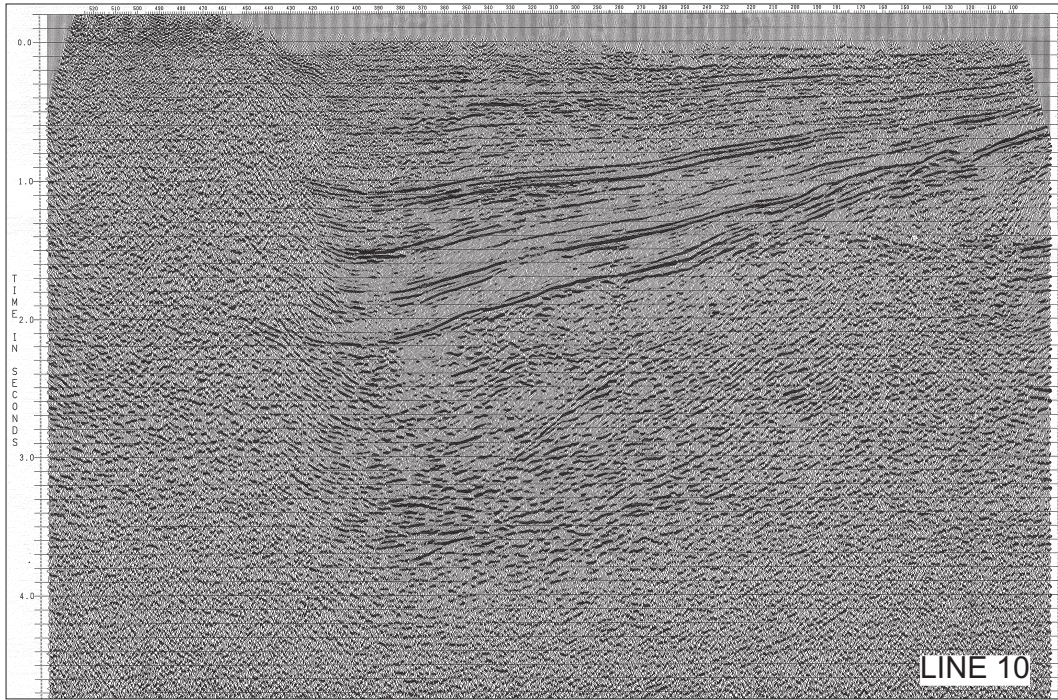


Figure 9. Uninterpreted and interpreted seismic section along line 10. MFZ- Malatya fault zone. See Figure 4b for location.

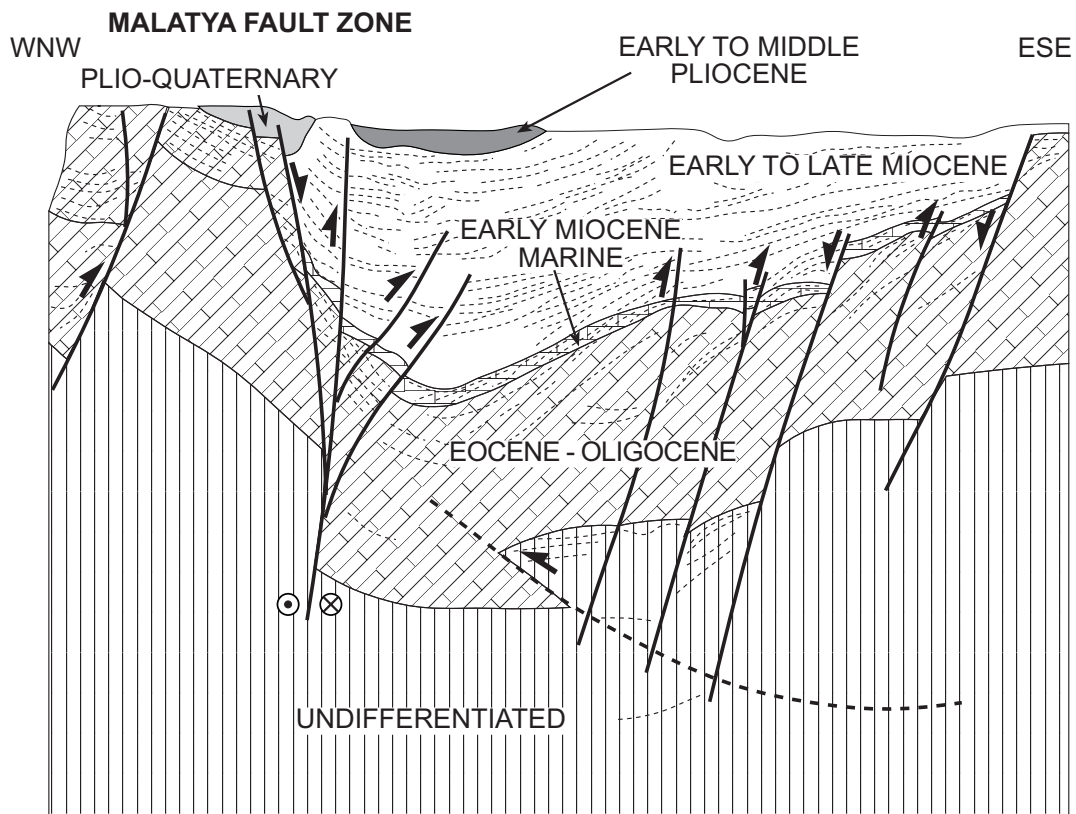
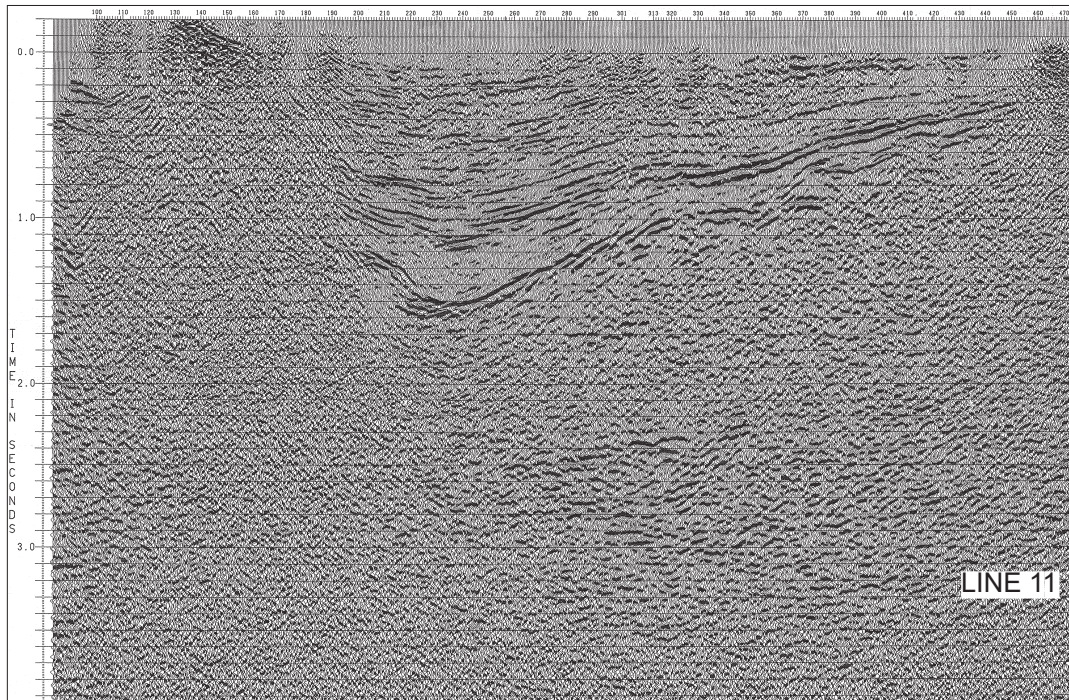


Figure 10. Uninterpreted and interpreted seismic section along line 11. MFZ– Malatya fault zone. See Figure 4b for location.

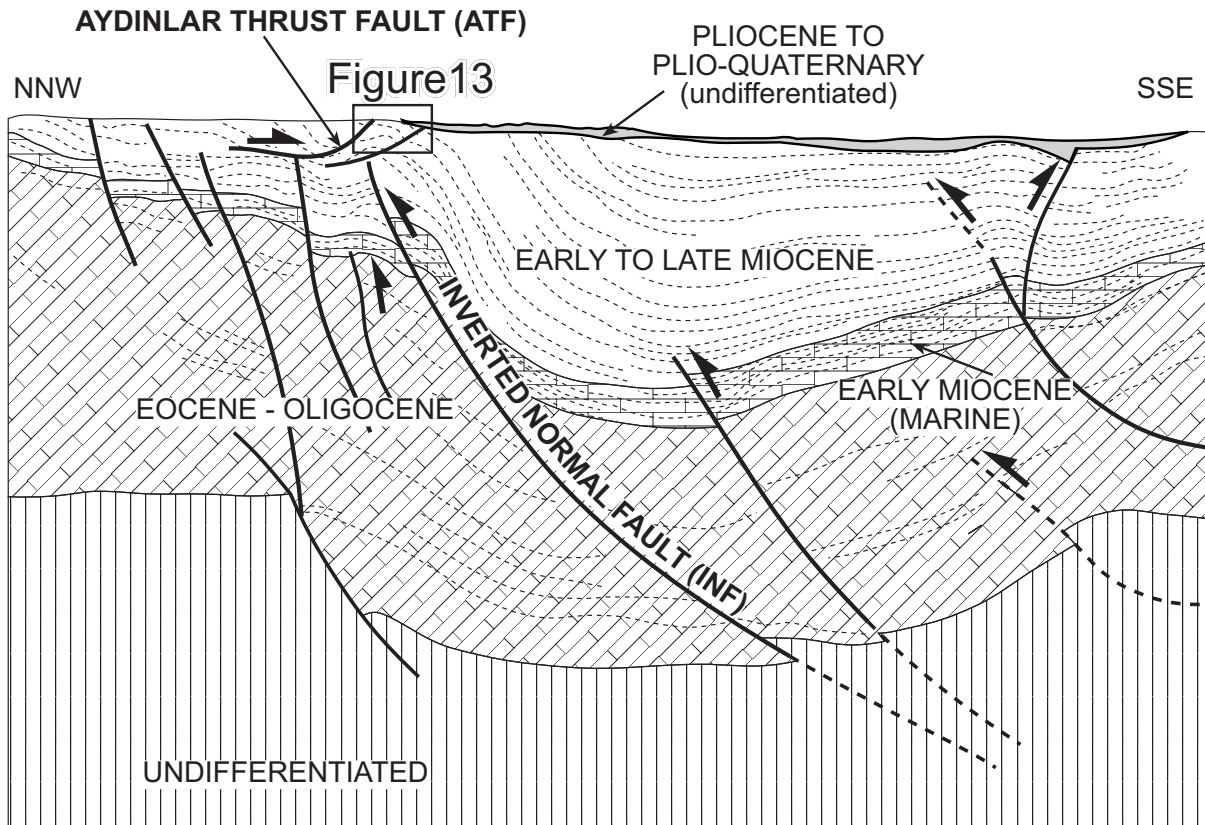
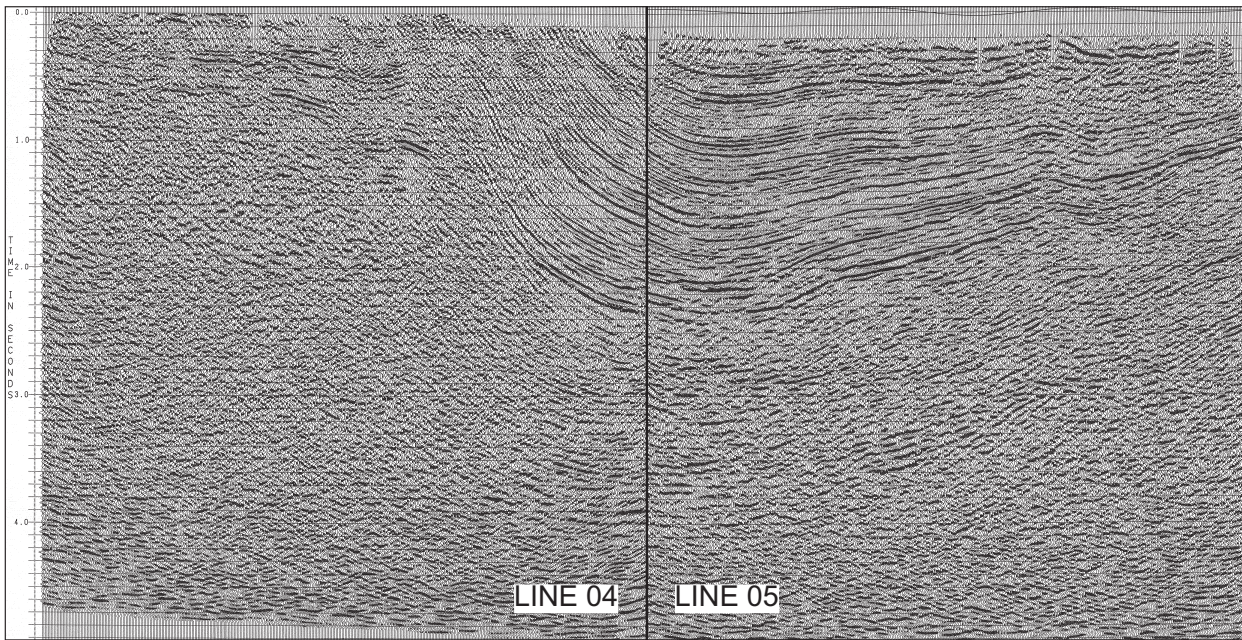


Figure 11. Uninterpreted and interpreted combined seismic section of lines 04 and 05. See Figure 4b for location.

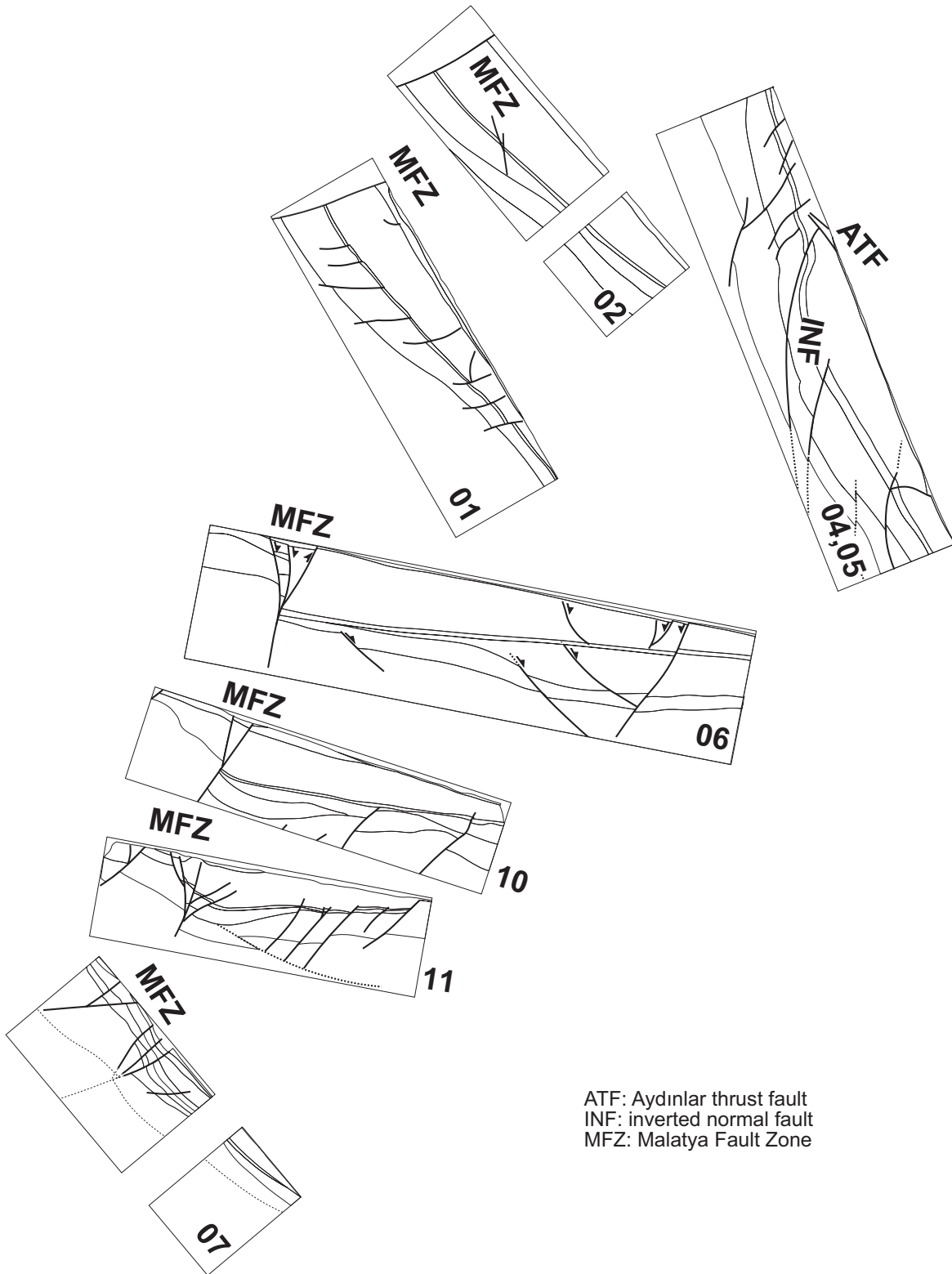


Figure 12. Simplified interpreted sections depicting 3D geometry of structures in the Malatya basin. INF: inverted normal fault. Note flower structure (terminology after Sylvester 1988) of the Malatya fault zone (MFZ).

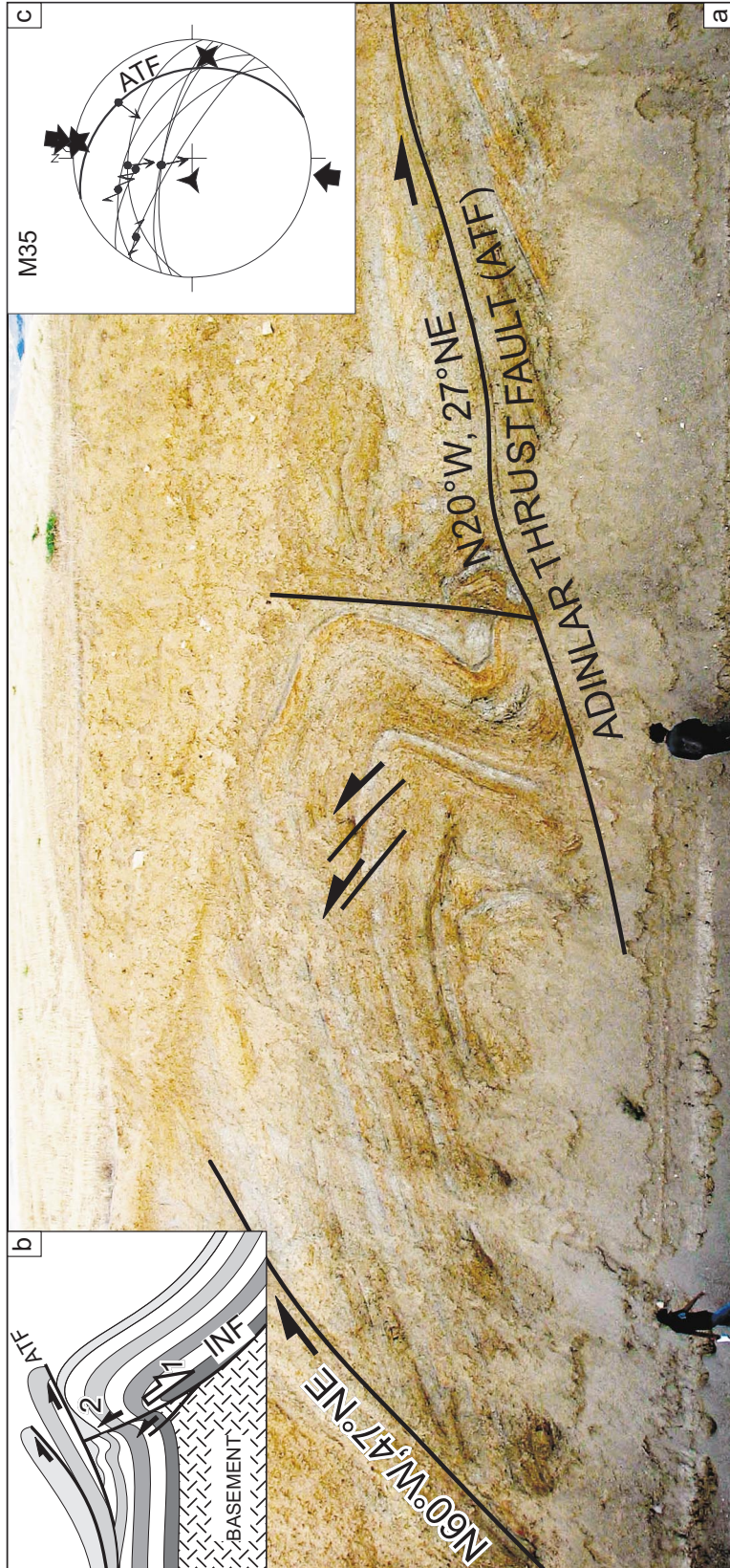


Figure 13. (a) View of exposed upper part of the Aydinlar thrust fault (ATF) developed within the Middle to Late Miocene units, showing the attitudes of the faults. Location is site 35; (b) a simplified model explaining the development of fault-bend fold, roof thrust (ATF) and triangular zone between the inverted normal fault (INF) and triangular fault (INF); (c) corresponding palaeostress configuration constructed using slickensides collected from the mesoscopic faults at the site.

In most areas of the Malatya Basin and all along the Malatya fault zone – from Doğanşehir in the south to İliç in the north (Figure 4b) – overprinting slickensides were observed. The primary slickensides, wherever observed, indicate normal faulting with a slight strike-slip component (pitches are not less than 60°), while at other localities, the dip-slip and strike-slip components vary among the sites. Based on this information, it is concluded that normal faulting pre-dated strike-slip deformation and that the oldest Neogene deformation in the region is extensional (phase 1). The mean orientation of the principal stresses, for deformation phase 1, is as follows: $\sigma_1=065^\circ\text{N}/88^\circ$, $\sigma_2=220^\circ\text{N}/02^\circ$, $\sigma_3=316^\circ\text{N}/02^\circ$. Having σ_1 vertical and other stresses horizontal indicates that deformation phase 1 was characterized by NW–SE-directed extension (Figure 14a).

The slickensides that marked deformation phase 1 were overprinted by another set of slickensides. Along the Malatya fault zone, some of the mesoscopic normal faults were reactivated as reverse faults. In addition, along the planes of these faults, overprinting slickensides are widespread. Based on these information, the overprinting slickensides are interpreted as a manifestation of a new phase of deformation (phase 2). The mean orientations of the principal stress for deformation phase 2 are as follows: $\sigma_1=354^\circ\text{N}/03^\circ$, $\sigma_2=244^\circ\text{N}/86^\circ$, $\sigma_3=080^\circ\text{N}/03^\circ$ (Figure 14b). Having σ_1 and σ_3 horizontal and σ_2 vertical indicates that strike-slip deformation prevailed during deformation phase 2.

In addition to overprinting slickensides along the normal faults mentioned above, overprinting slickensides were also observed within the Late Miocene to Pliocene units; at some of these sites, overprinting slickensides with relatively very low pitches (<15°), indicative of two different sets of strike-slip deformations, were observed. The newer slickensides generally indicate reverse components. In addition, similar slickensides were also observed in the Late Pliocene to Quaternary units (phase 3). The mean orientations of the principal stress are as follows; $\sigma_1=015^\circ\text{N}/15^\circ$, $\sigma_2=131^\circ\text{N}/53^\circ$, $\sigma_3=285^\circ\text{N}/34^\circ$ (Figure 14c). The orientations of the constructed palaeostress configurations indicate that in these sets σ_1 is horizontal while the orientations of σ_2 and σ_3 are variable (Fig 14c). At some of the sites, none of the principal stresses are vertical. In addition, the stress ratio (Φ) at these sites is quite low (Table 1). In consideration of the overprinting slickensides, the age of host lithology

and the very low Φ values, it is concluded that these sets indicate a new phase of deformation (phase 3). Very low Φ values are interpreted to be the result of equal or near equal magnitudes of σ_2 and σ_3 ; this results in stress permutations (Homberg *et al.* 1997) and coeval development of strike-slip and reverse faults, which is the case for phase 3. The plane of stress permutation has an attitude of N72°W, 82°SW and is indicated in Figure 14c. For the timing of deformation phases 2 and 3, refer to the next section.

Discussion

Evolution of the Malatya Basin

The evolution of the Malatya Basin was controlled mainly by three different phases of deformation during which the regional stress tensor changed; that in turn altered the style of deformation in the region. The first deformation phase occurred in the Early to Middle Miocene and caused the opening of the Malatya Basin. This deformation phase was accompanied by marine inundation in the region (Perinçek & Kozlu 1984; Sümengen & Uysal 1990). Although marine inundation may have been due to global sea-level rise, the presence of growth faults that controlled the deposition of the Early to Middle Miocene units is evidence for the opening of the Malatya Basin in the Early Miocene. The marine inundation suggests that the elevation of the Malatya Basin was at about sea level. The presence of shallow-marine algal limestones and the absence of deep marine deposits and fauna indicate that the Malatya Basin was not very deep during this time interval. The stratigraphic relationship of the Lower Miocene units with the Middle and Upper Miocene units is regressive. Marine conditions were replaced by continental ones in which lacustrine conditions dominated. It has been reported that there was a global sea-level drop in the Middle Miocene which resulted from a glacial event (cf. Hilgen *et al.* 1999); this implies that in the Middle Miocene, the region was not necessarily uplifted, although continental deposits dominated in this period. The Yamadağ volcanic rocks were extruded in the Early to Middle Miocene, which may also indirectly indicate that extensional conditions prevailed in the Early to Middle Miocene. Based on these information and assumptions, we conclude that extensional conditions commenced in the Early Miocene and lasted until the Late Miocene.

PHASE 1: EARLY TO MIDDLE MIOCENE EXTENSION

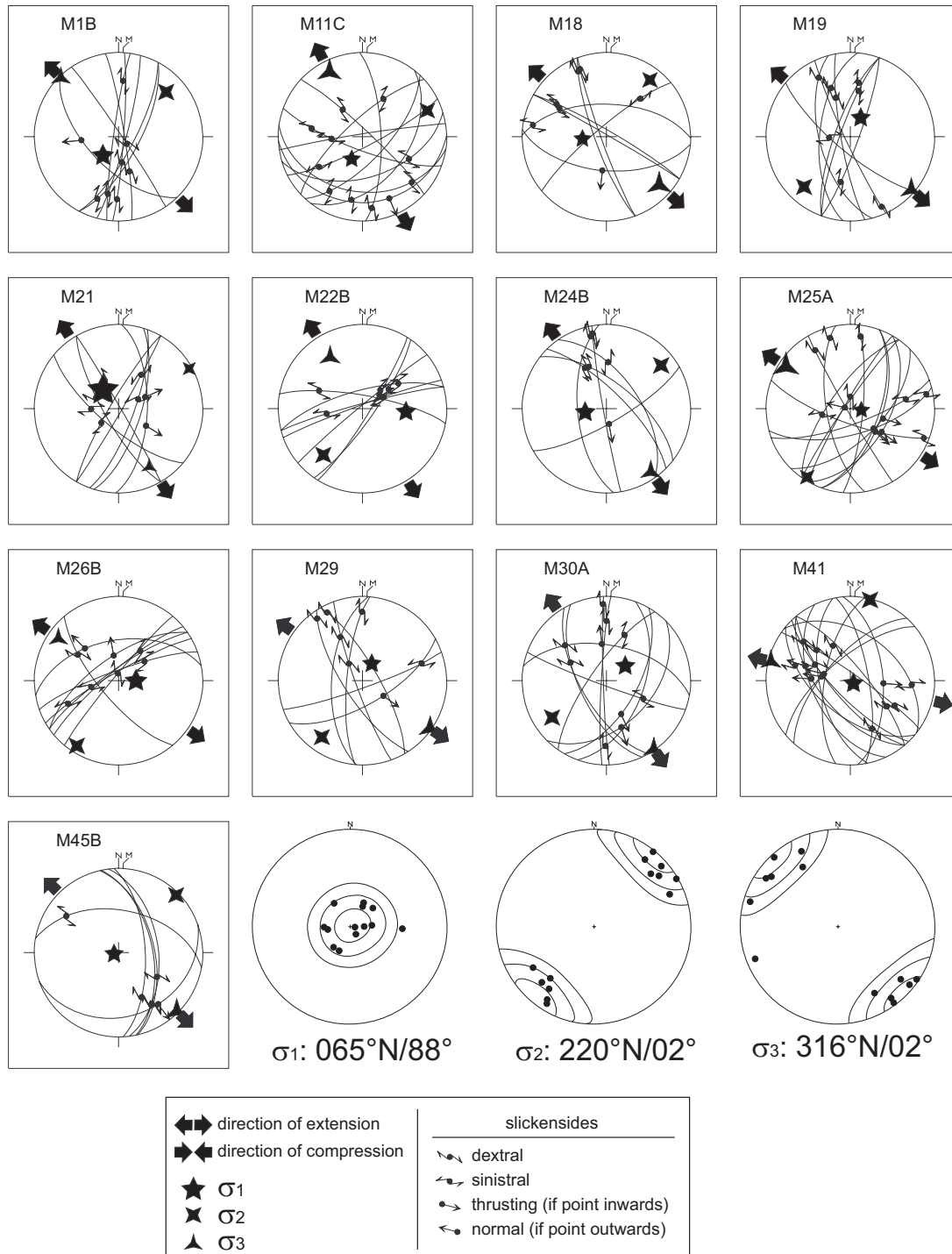


Figure 14. Palaeostress configurations and mean stress orientations determined from contour diagrams for each of the principal stress sets: (a) for phase 1; (b) for phase 2; (c) for phase 3. Note the interchanging (swapping) plane of σ_2 -and σ_3 -in phase 3.

PHASE 2: LATE MIOCENE - MIDDLE PLIOCENE COMPRESSION

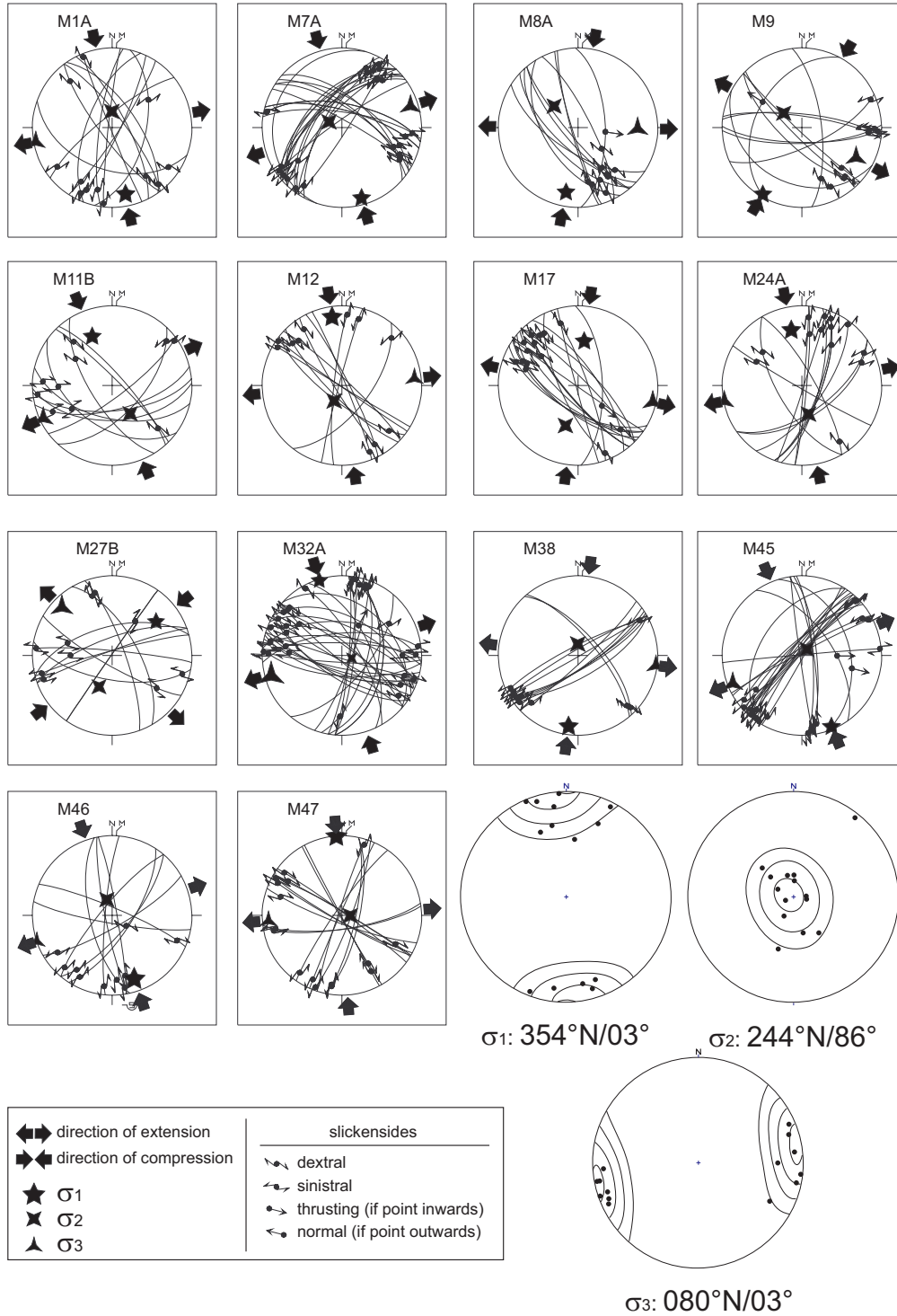


Figure 14b.

PHASE 3: PLIO-QUATERNARY COMPRESSION

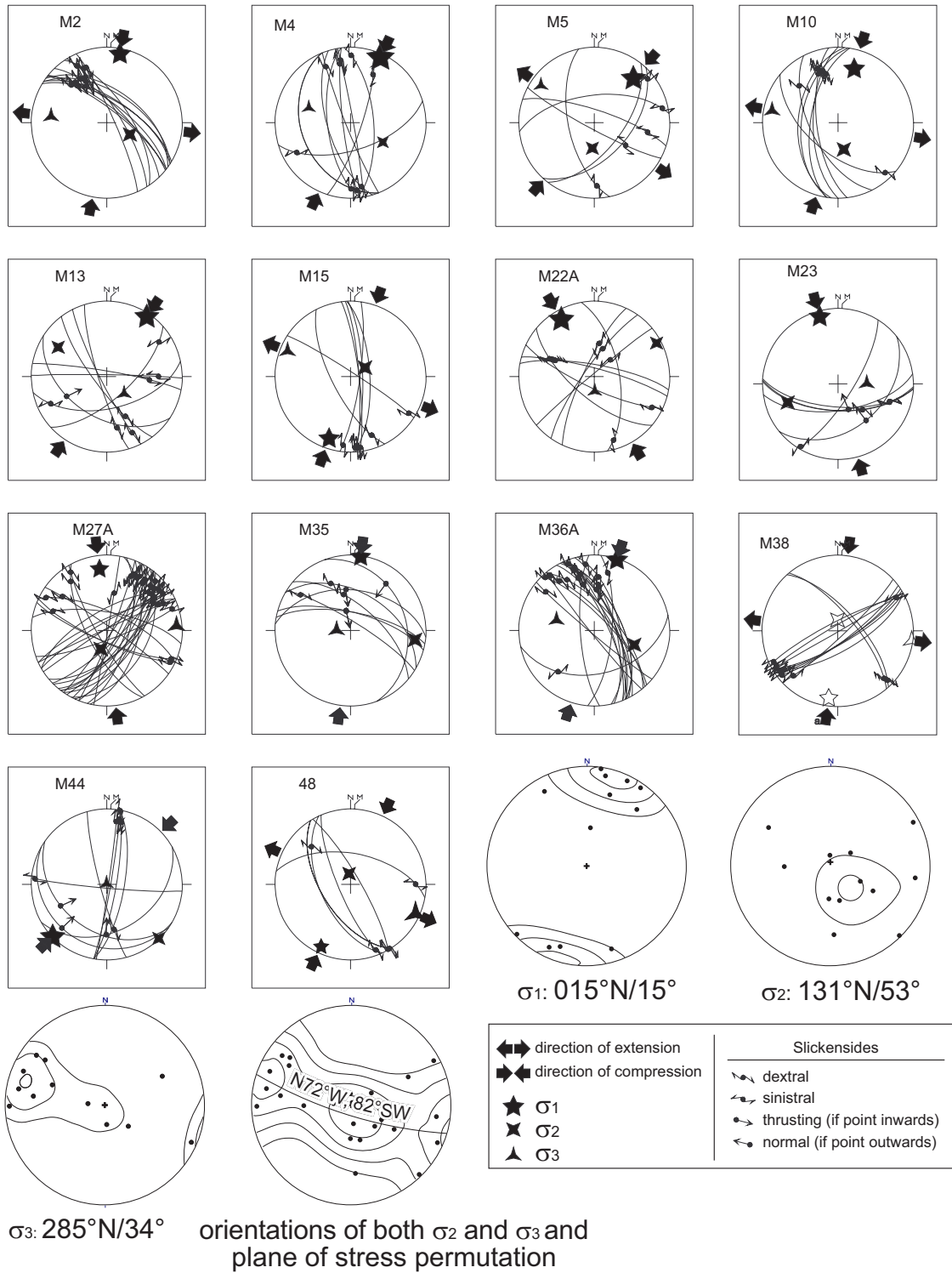


Figure 14c.

Table 1. Coordinates of the sample sites and corresponding palaeostress orientations.

Site Code	N	X	Y	σ_1 (D°/P°)	σ_2 (D°/P°)	σ_3 (D°/P°)	Φ
M1A	13	355021	4338743	169/16	359/74	259/3	0.56
M1B	8	355021	4338743	220/66	47/23	316/02	0.47
M2	11	368106	4336460	11/8	117/62	277/27	0.31
M4	10	384789	4326857	25/6	121/49	290/41	0.004
M5	6	387803	4324114	41/25	184/62	305/15	0.155
M7A	25	397206	4316636	164/9	294/76	73/11	0.629
M7B	9	397206	4316636	120/17	301/73	210/00	0.367
M8A	10	400894	4314465	191/19	312/57	91/26	0.643
M8B	8	400894	4314465	291/16	152/70	25/12	0.923
M9	11	411432	4288833	210/4	309/66	119/23	0.637
M10	7	417158	4286515	17/26	168/60	280/12	0.341
M11A	14	513988	4280832	309/69	130/21	40/00	0.511
M11B	10	513988	4280832	338/34	147/55	245/05	0.614
M11C	11	513988	4280832	206/66	68/18	333/15	0.761
M12	11	496422	4285258	352/14	207/73	84/09	0.473
M13	8	484149	4287686	34/5	301/26	134/64	0.163
M14	11	483017	4288173	231/77	330/02	61/13	0.836
M15	7	473295	4297850	199/14	58/72	292/11	0.375
M16	14	457498	4314619	107/71	02/05	270/19	0.158
M17	15	455629	4318427	008/43	197/46	102/05	0.615
M18	7	449344	4320217	265/67	37/16	132/16	0.775
M19	8	442246	4318017	028/69	223/20	131/05	0.618
M21	8	411749	4230108	321/66	060/04	152/23	0.008
M22A	8	399178	4222007	330/14	062/07	178/74	0.124
M22B	7	399178	4222007	094/47	220/29	328/29	0.564
M23	6	400610	4227599	164/13	269/50	064/37	0.318
M24A	13	408921	4246093	349/30	167/60	259/01	0.534
M24B	6	408921	4246093	261/69	052/18	145/09	0.55
M25A	13	405623	4249031	096/79	212/05	303/10	0.868
M25B	7	405623	4249031	153/83	313/07	044/02	0.647
M26A	11	426133	4241528	121/05	029/21	223/68	0.122
M26B	8	426133	4241528	090/73	213/09	305/14	0.427
M27A	30	435776	4236304	004/59	178/31	269/03	0.501
M27B	10	435776	4236304	337/01	238/82	067/07	0.741
M27C	11	435776	4236304	052/31	203/55	314/14	0.724
M28A	10	435925	4237093	138/67	263/14	357/19	0.344
M28B	7	435925	4237093	004/69	271/01	181/21	0.426
M29	7	443850	4244746	029/71	216/19	125/02	0.662
M30A	10	445973	4244680	052/67	236/23	145/02	0.595
M30B	8	445973	4244680	320/61	141/29	051/00	0.556
M31	8	483165	4253362	146/66	312/24	44/04	0.536
M32A	32	474115	4272863	343/05	102/80	252/09	0.629
M32B	10	474115	4272863	103/28	305/60	198/10	0.883
M35	7	441583	4277639	008/02	098/15	272/75	0.402
M36A	18	422317	4364543	018/02	110/43	286/47	0.307
M36B	10	422317	4364543	096/22	243/65	001/13	0.919
M38	11	455930	4348504	188/12	359/78	097/02	0.517
M41	14	421725	4277512	127/86	014/02	284/04	0.578
M42	9	420049	4278058	029/65	162/18	258/17	0.679
M44	9	410990	4289155	226/00	136/01	338/89	0.157
M45	23	413901	4298441	157/82	038/04	248/07	0.625
M45B	6	413901	4298441	255/86	45/ 4	135/2	0.685
M46	10	466840	4299107	161/17	341/73	251/00	0.347
M47	16	452331	4291609	356/01	091/81	266/09	0.402
M48	5	430992	4242799	205/10	352/781	114/06	0.795

N: Number of faults, X-Y: UTM Zone 37 coordinates of sites, D/P: Direction/Plunge, $\Phi = (\sigma_2 - \sigma_3) / (\sigma_1 - \sigma_3)$

It is generally accepted that the collision of the Arabian plate with the Eurasian plate took place by the end of the Middle Miocene (Şengör & Yılmaz 1981; Yılmaz *et al.* 1993; Westaway & Arger 2001; Westaway 2003 and references therein) and it is presumed that the Late Miocene was dominated by compressional deformation in the region. In the seismic sections and during field studies, no important (regional) unconformity was detected between the Middle Miocene and Upper Miocene units; however, the Late Miocene units in the Malatya Basin are dominated by fluvial red clastic materials. This has two implications: (1) the evolution of the Malatya Basin continued without break in its sedimentation in the Late Miocene, although a re-organization occurred in the regional stress field and, hence, in the deformation pattern; (2) extensional deformation lasted until the end of the Miocene and re-organization of the stress pattern and compressional deformation did not take place until the Pliocene, during which the Sultansuyu formation was deposited; this further implies that the effect of collision along the Bitlis-Zagros suture zone was not transferred until the Pliocene, or that the main collision occurred in the Pliocene. These questions are still debated and require further study. However, we favour the first assumption since the argument for Late Miocene collision is firmly established in the literature. Therefore, it is thought that deformation phase 2 commenced in the Late Miocene and resulted from collision of the Arabian plate with the Eurasian plate. The Late Miocene units are unconformably overlain by the Sultansuyu formation. Based on this information, it is proposed that deformation phase 3 commenced in the Late Pliocene and recently has still been in operation.

The geometry of the infill of the Malatya Basin is wedge-like in the E–W direction in which the western margin is thicker and the infill is thinning eastward, although sediment transport took place mainly from the eastern margin, as indicated by fore-set and shingle patterns in the seismic section (Figures 5–7). In the N–S direction, similar wedge-like geometry is also manifested in the seismic sections (Figure 11). There is a major step in the geometry of the Malatya Basin proximal to the Aydınlar thrust fault (ATF). The stepping is towards the south and corresponds to an inverted normal fault which facilitated an accommodation space for deposition of the Lower to Upper Miocene sequences. In addition, there are

a number of normal faults along which the southern blocks (hanging-wall blocks) displaced downward, indicating that the basin deepened from north to south and from west to east in the Early to Middle Miocene (deformation phase 2). Some of these normal faults were inverted during Late Miocene and Pliocene compressional events (deformation phases 2 and 3).

Malatya Fault Zone (MFZ)

As discussed previously, the Malatya and Ovacik fault zones are different segments of a single 'so called' Malatya-Ovacik fault zone (MOFZ, Koçyiğit & Beyhan 1998; Westaway & Arger 2001). In addition, Westaway & Arger (2001) postulated that the MOFZ was active 5–3 Ma and was a plate boundary between the Arabian and Anatolian plates which had taken up approximately 29 km of relative motion between them. They further speculated that after the development of the East Anatolian Fault Zone (EAFZ) as a single, through-going fault zone, the MOFZ became inactive. In addition to the seismic data, our observations about the Malatya fault zone are as follows. All along the escarpment at the western margin of the Malatya Basin (Figures 4a & 12), widespread mesoscopic faults with sinistral strike-slip and normal offset were observed (Figure 15). Such faults are observed all along the Malatya fault zone, especially in the area between Yazihan and Doğanşehir (see Figure 4 for their locations). These faults indicate stepping-down of the escarpment towards the Malatya Basin and the fault's reactivation. The Malatya fault zone is at least a 30-km-wide fault zone characterized by parallel to sub-parallel branches displaying an anastomosing pattern due to bifurcation and rejoining of different branches (Figures 4); it also has a positive flower-structure geometry in seismic sections, typical of strike-slip fault zones (cf. Sylvester 1988) (Figure 12). As discussed in the previous section, most of the observed mesoscopic faults have overprinting slickensides indicating at least three different phases of deformation. The first movement was characterized by a normal dip-slip component; other movement was dominantly strike-slip with reverse and normal components. Normal components in the later movements are observed mainly in the releasing bends, and reverse components were observed along the restraining bends of the major branches. Based on this information, we propose that the Malatya fault zone is a



Figure 15. Normal and sinistral mesoscopic faults developed along the Malatya fault zone near sites 24 & 25 (see Figure 2 for locations).

reactivated fault zone. It developed in the Early Miocene as a normal fault with a slight sinistral component and controlled the development of the Malatya Basin in the Early to Middle Miocene. That activity corresponds to deformation phase 1. Then, possibly in the Late Miocene and/or in the Pliocene, it that fault was reactivated and some of its normal branches were inverted; that activity corresponds to deformation phase 2. During this deformation phase, the Aydınlar thrust fault also developed and the Sultansuyu formation was deposited. In the post-Middle Pliocene, a regional reorganization in the stress field took place, corresponding to deformation phase 3. During this period, the Upper Plio–Quaternary units were deposited together with alluvial-fan deposits along the Malatya fault zone at the western margin of the Malatya Basin.

There is no direct evidence, such as medium- to large-magnitude earthquakes, along the Malatya fault zone. However, displaced stream courses (Figure 4) along the MFZ between Yazihan and Doğanşehir, the presence of a number of small-scale earthquakes as high as Ms 3.5, and a very prominent escarpment indicate that Malatya fault zone is presently active. These data imply that the Malatya fault zone is in a period of seismic quiescence. There is the possibility, therefore, that this fault zone might produce a large magnitude earthquake in the near future.

The other striking conclusion yielded by the seismic section is the lack of evidence for the Sultansuyu fault (Figure 4a), the presence of which was first proposed along the Sultansuyu River by Perinçek & Kozlu (1984), based on very persistent linearity of the river channel. Later Westaway & Arger (2001) discussed the same lineament. In line with our field observations, neither Perinçek & Kozlu (1984) nor Westaway & Arger (2001) have encountered any trace of faulting along the Sultansuyu River, despite its rectilinear course.

Ovacık Fault Zone (OFZ)

The Ovacık fault zone was first recognized by Arpat & Şaroğlu (1975), and was later studied by Aktimur (1979), Perinçek *et al.* (1987) and Chorowicz *et al.* (1994) using satellite images and aerial photos. Later, Koçyiğit & Beyhan (1998) proposed that the Ovacık and Malatya fault zones are two different segments of a single

Malatya-Ovacık fault zone (MOFZ), but without presenting any detailed supporting data. Westaway & Arger (2001) further speculated about the role of MOFZ in the evolution of the region based only on two observation points for the whole region, and on topographical and morphological information obtained from topographical maps. They also speculated that activity on the MOFZ ceased about 3 Ma, as mentioned previously

Our observations about the OFZ are as follows: (1) the OFZ is characterized by a number of fault segments less than 100 km length, and the zone bifurcates from the North Anatolian Fault Zone near the SE corner of the Erzincan Basin (Figure 4a), as discussed by Westaway & Arger (2001); (2) the escarpment that delimits the northern margin of the Ovacık Basin is the most prominent feature along the OFZ. Arpat & Şaroğlu (1975) argued that the segment of the OFZ at the northern margin of Ovacık Basin dips southward and has a normal component of slip which resulted in the formation of the Ovacık Basin; (3) different segments of the OFZ trend N70°E and are delimited in many places by quite prominent lineaments trending N20°E, parallel to the trend of the MFZ; (4) the Ovacık fault zone further bifurcates in the west starting at the western margin of the Ovacık Basin. The northernmost branch follows an approximately N80°W trend and is delimited in the west near Sandık by the Malatya fault zone. In the Malatya Basin, the OFZ is not constrained into a single fault zone; rather, it is distributed over a very large area, all of which is delimited in the west by the Malatya fault zone (Figure 16). In this area, almost all of the streams and the Euphrates River are deflected sinistrally. The maximum deflection is about 9.3 km near Dutluca (Figure 16a). Based on this deflection and some other morphotectonic data, Westaway & Arger (2001) argued that the maximum displacement of the OFZ is about 27 km. However, the sum of the deflections all along the different branches of the OFZ (Figure 4b) indicates a maximum displacement of not more than 20 km; (5) in addition, along one of the southernmost branches of the OFZ about 10 km east of Arguvan, a very pronounced anticline developed on the southern block of the fault (Fig 15b). In this area, it is observed that, this fault is a reactivated fault; it developed as a normal fault dipping south and later was reactivated as a sinistral strike-slip

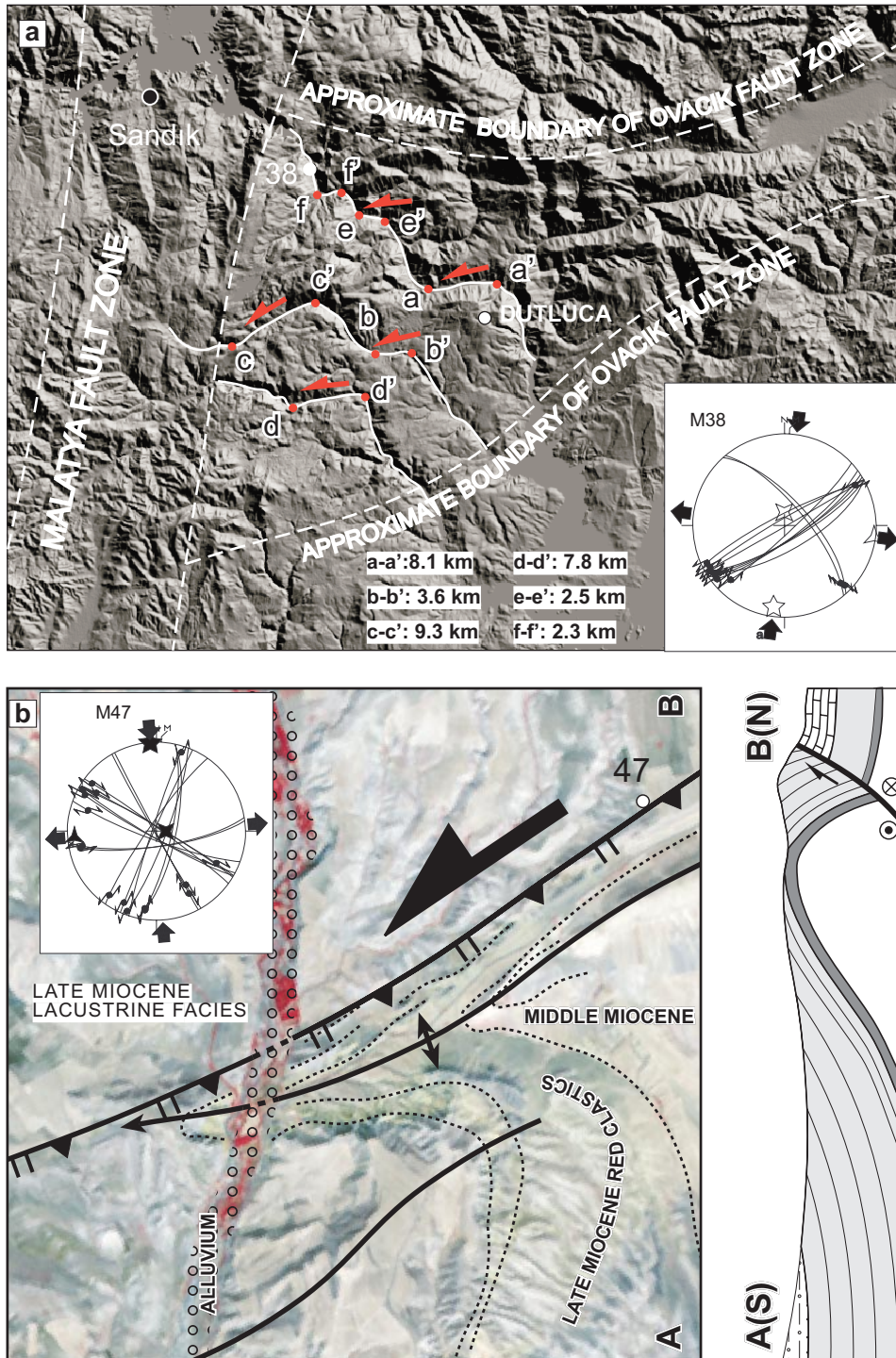


Figure 16. (a) Shaded relief image of the junction of the Malatya and Ovacik fault zones [marking major deflections in the streams (a-a' to f-f')] and the palaeostress configuration of site 38. Note that the Ovacik fault zone is delimited by the Malatya fault zone. Note also that the maximum deflection is 9.3 km; (b) simplified map and cross-section of the anticline on the hanging-wall block of an inverted normal fault overlaid on to ASTER image. See Figure 4b for location. This fault is one of the southernmost branches of the Ovacik fault zone.

fault with a reverse component. This implies that some of the pre-existing normal faults in the Early to Late Miocene (deformation phase 1) were reactivated in the successive deformation phases and were incorporated into different segments of the OFZ. Palaeostress data collected from this area, where the OFZ dominates, indicate that major compression was roughly N–S, which possibly drove the sinistral movement of the OFZ with a reverse component.

Briefly, the Ovacık fault zone is not a single through-going fault zone and is not only bifurcated into two branches around Arapkir, as proposed Westaway & Arger (2001). Rather, it developed in an area where very diffuse deformation is occurring. Moreover, the OFZ has a number of branches, some of which are reactivated normal faults with sinistral strike-slip components. Recent seismic activity along branches of the OFZ indicates that it is presently active.

All of this information invalidates the assumptions of Koçyiğit & Beyhan (1998) and Westaway & Arger (2001), and the kinematic model proposed by Westaway (2003). Therefore, current kinematic models for the Eurasian, Arabian and Anatolian plates should be revised.

Conclusions

This study leads us to the following conclusions:

1. Three different deformation phases have operated in and around the Malatya Basin: (a) The first phase was characterized by NW–SE-directed extension; (b) The second phase was characterized by approximately NNW–SSE-directed compression and a sub-vertical σ_2 , indicating the operation of transcurrent tectonics in the region; (d) The third phase was characterized by NNE–SSW-directed compression and variable vertical σ_2 and σ_3 orientations at various sites. It is interpreted that variable vertical stress indicates stress permutation between σ_2 and σ_3 , implying that the magnitudes of the intermediate and minor principal stresses were almost equal. The latest phase deformation (phase 3) involved transcurrent tectonics, commenced by the Late Pliocene, and is still active.
2. The Malatya Basin comprises infill ranging from Early Miocene to Recent in age.
3. Basin development was initiated in deformation phase 1 (in the Early Miocene) and continued until the Late Miocene without any significant hiatuses. Basin development was accompanied by normal faulting, during which the Malatya fault zone was also a normal fault zone.
4. The Malatya Basin displays a wedge-like geometry in the E–W and N–S directions, and has a major step in the north proximal to the Aydınlar thrust fault.
5. The Malatya and Ovacık faults are two independent fault zones *contra* Koçyiğit & Bayhan (1998) and Westaway & Arger (2001), who proposed that they are a single fault zone, the ‘so-called’ Malatya-Ovacık fault zone.
6. Both the Malatya and Ovacık fault zones are presently active, *contra* Westaway & Arger (2001) who proposed that they become inactive about 3 Ma.
7. Most of the faults, including the Malatya and some branches of the Ovacık fault zones, are reactivated pre-existing faults which developed as normal faults in the Early to Late Miocene and reactivated as sinistral strike-slip faults, possibly during later compressional events in the post-Middle Miocene.
8. Current kinematic models for the Eurasian, Arabian and Anatolian plates should be revised on the basis of the data presented here.
9. The seismic potential of the Malatya and Ovacık faults should be assessed in detail since they have the potential of producing large earthquakes in the near future.

Acknowledgement

This study was supported by the “Middle East Basins Evolution” Programme, project no. MEBE 16-02 (CNRS-France). We are thankful to Eric Barrier who encouraged us to take part in the MEBE Program and critically reviewed the field reports. Hans de Bruijn, Gerçek Saraç, Engin Ünay, and Erksin Güleç are thanked for the dating of the fossils and for generously sharing their mammal-fossil database of Turkey. Cengiz Demirci provided seismic sections.

References

- AKTAŞ, G. & ROBERTSON A.H.F. 1984. The Maden complex, SE Turkey: evolution of a Neotethyan active margin. In: DIXON J.E. & ROBERTSON, A.H.F. (eds), *The Geological Evolution of the Eastern Mediterranean*. Geological Society, London, Special Publications 17, 375–402.
- AKTİMUR, S. 1979. *Malatya-Sivas Dolayının Uzaktan Algılama Yöntemi ile Çizgiselliklerinin İncelenmesi [The Lineament Analysis of Malatya-Sivas Region Using Remote Sensing]*. MTA Report No. 6651 [unpublished].
- ANGELIER, J. 1988. *Tector: Determination of Stress Tensor Using Fault Slip Data Set*. Quantitative Tectonics, University Pierre and Marie Curie, Paris.
- ANGELIER, J. 1994. Fault slip analysis and palaeostress reconstruction. In: HANCOCK, P.L. (ed), *Continental Deformation*. Pergamon Press, Oxford, 53–100.
- ARGER, J., MITCHELL J. & WESTAWAY, R. 2000. Neogene and Quaternary volcanism of south-eastern Turkey. In: BOZKURT, E., WINCHESTER, J.A., PIPER, J.D.A. (eds), *Tectonics and Magmatism, in Turkey and the Surrounding Area*. Geological Society, London, Special Publications 173, 459–487.
- ARPAT, E. & ŞAROĞLU, F. 1975. Türkiye'deki bazı önemli genç tektonik olaylar [Some recent tectonic events in Turkey]. *Türkiye Jeoloji Kurumu Bülteni* 18, 91–101.
- BİNGÖL, A.F. 1984. Geology of the Elazığ area in the eastern Taurus region. In: TEKELİ, O. & GÖNCÜOĞLU, M. (eds), *Geology of the Taurus Belt*. Mineral Research and Exploration Institute (MTA) Publication, Ankara, Turkey, 209–216.
- CHOROWICZ, J., LUXEY, P., LYBERIS, N., CARVALHO, J., PARROT, J.-F., YÜRÜR, T. & GÜNDOĞDU, M.N. 1994. The Maras Triple Junction (southern Turkey) based on digital elevation model and satellite imagery interpretation. *Journal of Geophysical Research* 99/B10, 20225–20242.
- DEWEY, J.F., HEMPTON, M.R., KIDD, W.S.F., ŞAROĞLU, F. & ŞENGÖR, A.M.C. 1986. Shortening of continental lithosphere: the neotectonics of Eastern Anatolia – a young collisional zone. In: COWARD, M.P. & RIES, A.C. (eds), *Collision Tectonics*. Geological Society, London, Special Publications 19, 3–36.
- GENÇALIOĞLU-KUŞÇU, G., GÖNCÜOĞLU, M.C. & KUŞÇU, İ. 2001. Post-collisional magmatism on the northern margin of the Taurides and its geological implications: geology and petrology of the Yahyalı-Karamadazi granitoid. *Turkish Journal of Earth Sciences* 10, 103–119.
- GÖRÜR, N., OKTAY, F.Y., SEYMEY, İ. & ŞENGÖR, A.M.C. 1984. Palaeotectonic evolution of the Tuzgözü basin complex, central Turkey: sedimentary record of a Neotethyan closure. In: DIXON, J.E. & ROBERTSON, A.H.F. (eds), *The Geological Evolution of the Eastern Mediterranean*. Geological Society, London, Special Publications 17, 77–112.
- HARDCASTLE, K.C. & HILLS, L.S. 1991. Brute3 and Select: QuickBasic 4 programs for determination of stress tensor configurations and separation of heterogeneous populations of fault-slip data. *Computers and Geosciences* 17, 23–43.
- HILGEN, F. J., ABDUL-AZIZ, H., KRIJGSMAN, W., LANGEREIS, C.G., LOURENS, L.J., MEULENKAMP, J.E., RAFFI, I., STEENBRINK, J., TURCO, E., VAN VUGT, N., WIJBRANS, J. R. & ZACHARIASSE, W.J. 1999. Present status of the astronomical (polarity) time-scale for the Mediterranean Late Neogene. *Philosophical Transactions Royal Society London A* 357, 1931–1947.
- HOMBERG, C., HU, J.C., ANGELIER, J., BERGERAT, F. & LACOMBE, O. 1997. Characterization of stress perturbation near major fault zones: insights from 2-D distinct-element numerical modeling and field studies (Jura Mountains). *Journal of Structural Geology* 19, 703–718.
- JAFFEY, N. & ROBERTSON, A.H.F. 2004. Non-marine sedimentation associated with Oligocene–Recent exhumation of the Central Taurus Mountains, S. Turkey. *Sedimentary Geology* 173, 53–89.
- KAYMAKCI, N. 2000. *Tectono-stratigraphical Evolution of the Çankiri Basin (Central Anatolia, Turkey)*. PhD Thesis, Geologica Ultraiectina. No. 190, Utrecht University Faculty of Earth Sciences, The Netherlands, ISBN 90-5744-047-4.
- KAYMAKCI, N., WHITE, S.H. & VAN DIJK P.M. 2000. Palaeostress inversion in a multiphase deformed area: kinematic and structural evolution of the Çankiri Basin (central Turkey), Part 1. In: BOZKURT, E., WINCHESTER, J.A. & PIPER, J.A.D. (eds), *Tectonics and Magmatism in Turkey and the Surrounding area*. Geological Society London Special Publication 173, 445–473.
- KAYMAKCI, N., DUERMEIJER, C.E., LANGEREIS, C., WHITE, S.H. & VAN DIJK, P.M. 2003b. Oroclinal bending due to indentation: a paleomagnetic study for the early Tertiary evolution of the Çankiri Basin (central Anatolia, Turkey). *Geological Magazine* 140, 343–355.
- KAYMAKCI, N., WHITE, S.H. & VAN DIJK P.M. 2003a. Kinematic and structural development of the Çankiri Basin (central Anatolia, Turkey): a palaeostress inversion study. *Tectonophysics* 364, 85–113.
- KOÇYİĞİT, A. & ALTINER, D. 2002. Tectonostratigraphic evolution of the North Anatolian palaeorift (NAPR): Hettangian-Aptian passive continental margin of the northern Neo-Tethys, Turkey. *Turkish Journal of Earth Sciences* 11, 169–191.
- KOÇYİĞİT, A. 1991. An example of an accretionary forearc basin from north central Anatolia and its implications for the history of subduction of Neotethys in Turkey. *Geological Society America Bulletin* 103, 22–36.
- KOÇYİĞİT, A. & BEYHAN, A. 1998. A new intracontinental transcurrent structure: the Central Anatolian Fault Zone, Turkey. *Tectonophysics* 284, 317–336.
- KOZLU, H. 1987. Misis-Andırın dolayının stratigrafisi ve yapısal evrimi [Stratigraphy and structural evolution of Misis-Andırın region]. *Türkiye 7. Petrol Kongresi, Bildiriler Kitabı*, 104–116.
- LEO, G.W., MARVIN, R.F. & MEHNERT H.H. 1974. Geologic framework of the Kuluncak-Sofular area, east-central Turkey, and K-Ar ages of igneous rocks. *Geological Society America Bulletin* 85, 1785–1788.

- ÖZGÜL, N. 1976. Torosların bazı temel jeolojik özellikleri [Basic geologic characteristics of Taurides]. *Türkiye Jeoloji Kurumu Bülteni* **19**, 65–78.
- ÖZGÜL, N. & TURŞUCU A. 1984. Stratigraphy of the Mesozoic carbonate sequence of the Munzur Mountains (eastern Taurides). In: TEKELİ, O. & GÖNCÜOĞLU, M. (eds), *Geology of the Taurus Belt*. General Directorate of Mineral Research and Exploration (MTA), Special Publication, Ankara, Turkey, 173–180.
- PERİNÇEK, D. & KOZLU, H. 1984. Stratigraphy and structural relations of the units in the Afşin-Elbistan-Doğuşehir region (eastern Taurus). In: TEKELİ, O. & GÖNCÜOĞLU, M. (eds), *Geology of the Taurus Belt*. General Directorate of Mineral Research and Exploration (MTA), Special Publication, Ankara, Turkey, 181–198.
- PERİNÇEK, D., GÜNAY, Y. & KOZLU, H. 1987. Doğru ve güneydoğu Anadolu bölgesindeki yanar atımlı faylar ile ilgili yeni gözlemler [New observations on the strike-slip faults of east and southeast Anatolia]. *Türkiye 7. Petrol Kongresi Bildiriler Kitabı*, 89–103.
- ROBERTSON, A.H.F. 2002. Overview of the genesis and emplacement of Mesozoic ophiolites in the eastern Mediterranean Tethyan region. *Lithos* **65**, 1– 67.
- ROBERTSON, A.H.F., ÜNLÜGENÇ, U., İNAN, N. & TASLI, K. 2004. The Misis–Andirin complex: mid-Tertiary subduction/accretion and melange formation related to closure and collision of the South-Tethys in S Turkey. *Journal of Asian Earth Sciences* **22**, 413–453.
- ROJAY, B., YALINIZ, M.K. & ALTINER, D. 2001. Tectonic implications of some Cretaceous pillow basalts from the North Anatolian ophiolitic mélangé (central Anatolia-Turkey) to the evolution of Neotethys. *Turkish Journal of Earth Sciences* **10**, 93–102.
- SARAÇ, G., DE BRUIJN, H., GÜLEÇ, E., ÜNAY, E. WHITE, T. & VAN MEULEN, A. 2000. *Türkiye Omurgalı Fosil Yatakları [Mammalian Fossils of Turkey]*. MTA Report [unpublished]
- ŞENGÖR, A.M.C. & YILMAZ, Y. 1981. Tethyan evolution of Turkey: a plate tectonic approach. *Tectonophysics* **75**, 181–241.
- ŞENGÖR, A.M.C., YILMAZ, Y. & SUNGURLU, O. 1984. Tectonics of the Mediterranean Cimmerides: nature and evolution of the western termination of palaeo-Tethys. In: DIXON, J.E. & ROBERTSON, A.H.F. (eds), *The Geological Evolution of the Eastern Mediterranean*. Geological Society, London, Special Publications **17**, 77–112.
- ŞENGÖR, A.M.C., ŞAROĞLU, F. & GÖRÜR, N. 1985. Strike-slip deformation and related basin formation in zones of tectonic escape: Turkey as a case study. In: BIDDLE, K.T. & CHRISTIE-BLICK, N. (eds), *Strike-Slip Deformation Basin Formation and Sedimentation*. Society of Economic Paleontologists and Mineralogists, Special Publication **37**, 227–264.
- SICKENBERG, O. 1975. Die Gliederung des höheren Jungtertiärs und Altquartärs in der Türkei nach Vertebraten und ihre Bedeutung für die internationale Neogen-Stratigraphie. *Geologisches Jahrbuch* **15**, 1094–1116.
- SÜMENGİN, M. & UYSAL, Ş. 1990. *Ağzıkara Project. Petroleum Potential of Kayseri-Gürün-Kahramanmaraş-Malatya Region*. Mobil Exploration Mediterranean Inc. Report [unpublished].
- SYLVESTER, A.G. 1988. Strike-slip faults. *Geological Society America Bulletin* **100**, 1666–1703.
- ÜNAY, E. & BRUIJN, H. 1998. Plio-Pleistocene rodents and lagomorphs from Anatolia. *Proceedings of SEQS-EuroMam Symposium* **60**, 432–485.
- WESTAWAY, R. 2003. Kinematics of the Middle East and eastern Mediterranean updated. *Turkish Journal of Earth Sciences* **12**, 5–46.
- WESTAWAY, R. & ARGER, J. 2001. Kinematics of the Malatya–Ovacık fault zone. *Geodinamica Acta* **14**, 103–131.
- YALÇIN, M.N. & GÖRÜR, N. 1984. Sedimentological evolution of the Adana Basin. In: TEKELİ, O. & GÖNCÜOĞLU, M.C. (eds), *Geology of the Taurus Belt*. General Directorate of Mineral Research and Exploration (MTA) Special Publication, 165–172.
- YALINIZ, M.K. & GÖNCÜOĞLU, M.C. 1999. Clinopyroxene compositions of the isotropic gabbros from the Sarıkaraman Ophiolite: new evidence on supra-subduction zone type magma genesis in central Anatolia. *Turkish Journal of Earth Sciences* **8**, 103–112.
- YAZGAN, E. 1984. Geodynamic evolution of the Eastern Taurus region. In: TEKELİ, O. & GÖNCÜOĞLU, M.C. (eds), *Geology of the Taurus Belt*. General Directorate of Mineral Research and Exploration (MTA) Special Publication, 199–208.
- YILMAZ, Y., YİĞİTBAŞ, E. & GENÇ, C.Ş. 1993. Ophiolitic and metamorphic assemblages of southeast Anatolia and their significance in the geological evolution of the orogenic belt, *Tectonics* **12**, 1280–1297.

Received 23 February 2005; revised typescript accepted 03 January 2006